CONTRACT NAS 8-18037

ANALYTICAL STUDY OF NONMETALLIC PARTS FOR LAUNCH VEHICLES AND SPACECRAFT STRUCTURES

Quarterly Progress Report Number 2
Covering Period
October 1, 1966 through January 1, 1967

Prepared by

THE BOEING COMPANY
Space Division
Seattle, Washington

C. F. Tiffany - Program Supervisor
D. H. Bartlett - Program Leader

Prepared for

NATIONAL AERONAUTICS AND SPACE ADMINISTRATION
George C. Marshall Space Flight Center
Huntsville, Alabama

THE **BOEING** COMPANY AEROSPACE GROUP

SPACE DIVISION · KENT FACILITY P.O. BOX 3868 · SEATTLE, WASHINGTON 98124

January 5, 1967

2-1101-94-3-76-OR
9-4-4541

National Aeronautics and Space Administration
George C. Marshall Space Flight Center
Huntsville, Alabama 35812

Attention: PR-SC

Subject: Contract NAS 8-18037 - "Analytical Study of Non-Metallic Parts for Launch Vehicles and Spacecraft Structures)
Quarterly Progress Report No. 2

Gentlemen:

The Boeing Company transmits herewith one (1) copy of its Quarterly Progress Report No. 2 in accordance with Section III of Exhibit "A" to the subject contract.

Sincerely,

THE BOEING COMPANY
Space Division

F. P. Syverson
Contracts Manager
Space Research and Development

Enclosure:
Quarterly Progress Report No. 2 (1)

cc:
MS-IL (1)
MS-T (1)
MS-IP (2)
R-P&VE-SAA (9 copies and 1 reproducible)
(Carl A. Loy)
LeRC (1)
SEG/MAAE (1)
(T. J. Reinhart, Jr.)

FOREWORD

This report presents work accomplished by the Boeing Company during the second quarter October 1, 1966 to January 1, 1967 on an "Analytical Study of Nonmetallic Parts for Launch Vehicles and Spacecraft Structures", NASA Contract NAS 8-18037. Also included is a summarization of work accomplished during the first three months of the program which was previously reported in Quarterly Progress Report #1. The work is administered by the George C. Marshall Space Flight Center, P&VE Laboratory, Huntsville, Alabama. The NASA Technical Leader is Mr. Carl A. Loy.

Performance of this contract is under the direction of the Structural Development Unit, Spacecraft Mechanics and Materials Technology, Space Division of the Boeing Company. Mr. C. F. Tiffany is Program Supervisor and Mr. D. H. Bartlett is Program Leader.

NOTE

Because this is a progress report, information contained herein is tentative and subject to changes, corrections, and modifications.

1.0 INTRODUCTION

The objective of this investigation is to determine the applicability of fiber reinforced plastics in spacecraft and launch vehicle structural components, with particular interest in the use of this type of structure to support cryogenic tanks. An additional objective is to compare the merit of these components with metallic parts of the same functional design. A survey of literature from past and current programs will be made to assemble information such as properties and methods of fabrication essential to the design phase. Parts will be designed utilizing the inherent advantages of reinforced plastic structure and comparisons made with designs of metallic parts. A quantity of parts will be fabricated and subjected to destruction tests intended to prove their suitability for the application selected.

During the first reporting period (July 1 to October 1, 1966) a literature survey was completed, structural composite properties were selected for design and three types of structural elements were chosen for design, fabrication and test. The structural elements selected were (1) tension members for cryogenic tank supports, (2) combined compression and tension struts for cryogenic tank supports, and (3) beams for payload packages (noncryogenic). Two tension rod configurations were selected for study; these were flat members with laminated metal foils for increased bearing strength, and round members incorporating a wedging feature at the end attachments. Compression struts in the length range of 20 to 30 inches were configured as cylindrical tubes of reinforced plastic construction bonded to metallic end fittings. It was found that significant weight savings in fiberglass compression struts are available when compared with metallic parts, if high loading is considered, i.e., 12,000 lbs or more for a 20 inch member; however, in any load range, the fiberglass parts consistently provide the least heat leak due to the low thermal conductivity of the composite. Beams with sandwich web, stiffened web and truss webs were investigated and the sandwich web approach was selected as providing the least weight design in the span lengths of interest.

The reinforcement selected for all designs was S-994 fiberglass in either multiple end rovings, cloth or single end yarn. A variety of acceptable resin systems were identified in the literature survey, the preferred being Epon 826 (for wet winding) and E-787 prepreg. Structural composite properties for design were selected from results of the Reference 1 contract.

A detailed presentation of study results and a discussion of the analytical approach is contained in the first Quarterly Report.

2.0 SUMMARY OF WORK ACCOMPLISHED

During the fourth and fifth months, the detailed designs of flat and round tension rods and a compression strut were developed. A titanium tension rod and a titanium compression strut were also designed using the same loads as for the nonmetallic parts to allow heat flow comparisons. The design drawings for the titanium parts are not complete, hence they are not included in this report. The beam optimization computer program was initiated and has produced data on depths, cross section geometry and weight for a variety of spans and loading.

During the sixth month, the test plans for tension rods and compression struts were prepared and coordinated with the MSFC Technical Leader, and material orders were placed for fiberglass, epoxy resin, adhesives, and the required metallic materials. The manufacturing methods were selected and tool design started. The analysis of aluminum beams for comparison with the nonmetallic parts was completed. Comparisons of the two types of beams show the span and loading range where fiberglass construction offers weight savings over aluminum construction.

A detailed discussion of the designs, fabrication approach, and test plans follows.

Tension Rods

Figure 1 is the design drawing of a flat tension rod with metal foils laminated into the composite at the ends to provide bearing strength. On the left hand side of the drawing, the tension rod is shown in place on a cryogenic tank assembly. This view serves to show the clearances required for this type of member, an important feature when round rods are considered. The parts are fabricated by winding 12 end fiberglass roving impregnated with an Epon 826 resin system on a flat frame. The stainless steel foils are coated with adhesive and placed between appropriate layers of windings. The entire frame assembly is then vacuum bagged and cured. After cure, the composite with integral metal foils is cut from the frame, the edges are trimmed and the tension rods produced by cutting parallel strips of the required width. The type of cutting wheel and speeds employed is critical to obtaining a smooth edge with a minimum of fiber damage. A hole of the required size may then be drilled in each end for attachment. The pins used for attachment are required to have a bearing strength nearly equivalent to the foil material and should be made from an alloy considered suitable for cryogenic service. The A286 alloy selected for these pins meets both these requirements. An alternate material would be Inconel 718 cold reduced and aged to a minimum tensile strength above 200,000 psi.

Figure 2 is the design drawing of a circular tension rod which also incorporates thin metal foils for increased bearing strength at end attachments. The diameter at the ends as well as the width of the flat tension rods is a function of both the number of foils and the adhesive bond strength. In the case of the flat rods it was relatively easy to add foils if necessary, the only undesirable effect being increased thickness. However, in the case of the circular rods, the design shown represents a minimum diameter for the internal attachment lug so the use of additional foils would only increase outside diameter resulting in the need to shorten the fiberglass section to avoid interference with the pressure vessel. In all the tension rod designs shown, a single bolt serves as the attachment at each end. This approach eliminates the uncertainties of load transfer attendant with multiple fasteners. A design requirement of the circular as well as the flat rods was that the bearing stress in the foils be below the yield strength of the material at design ultimate load. This is believed necessary to eliminate any prying

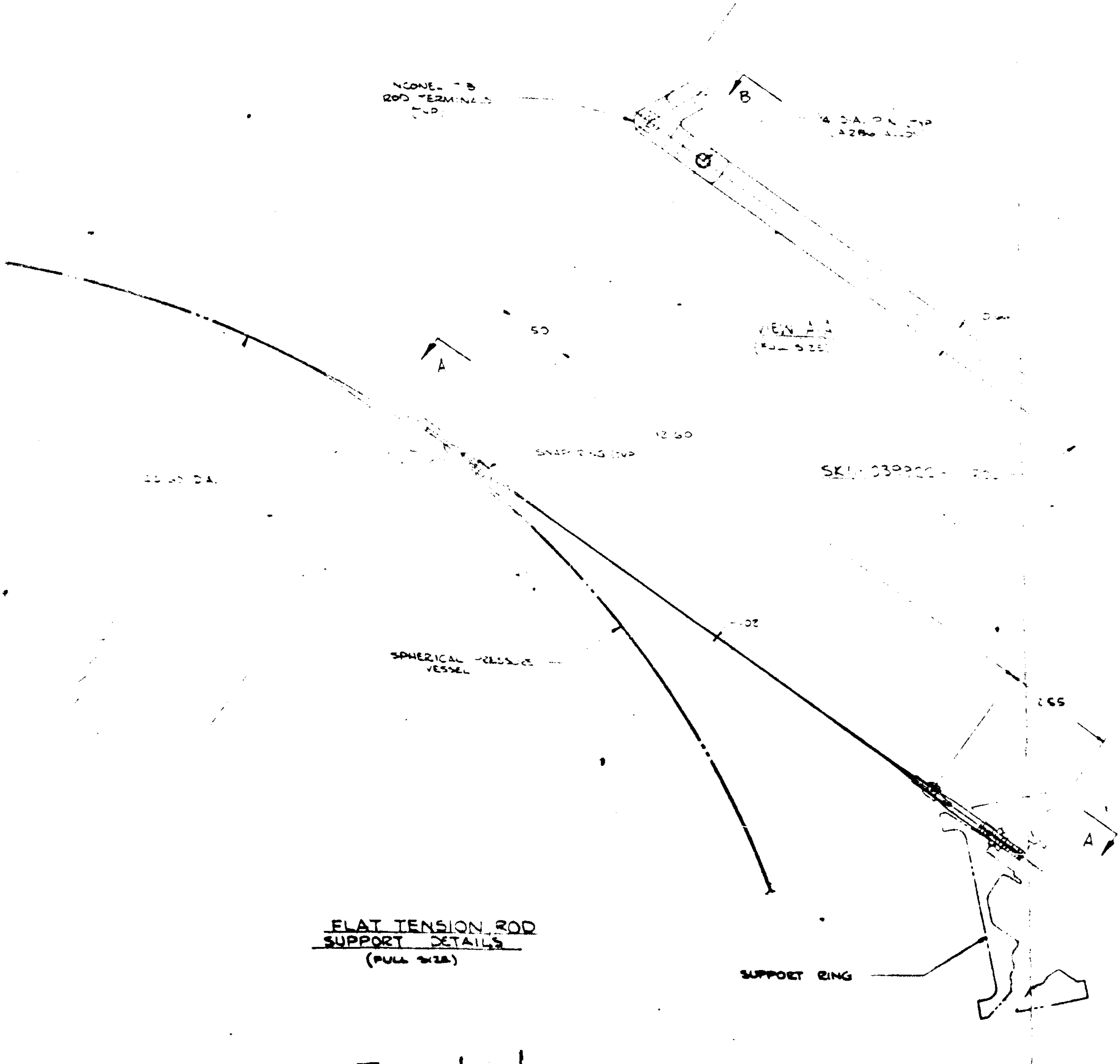

FLAT TENSION ROD
SUPPORT DETAILS
(FULL SIZE)

FIG-1-1

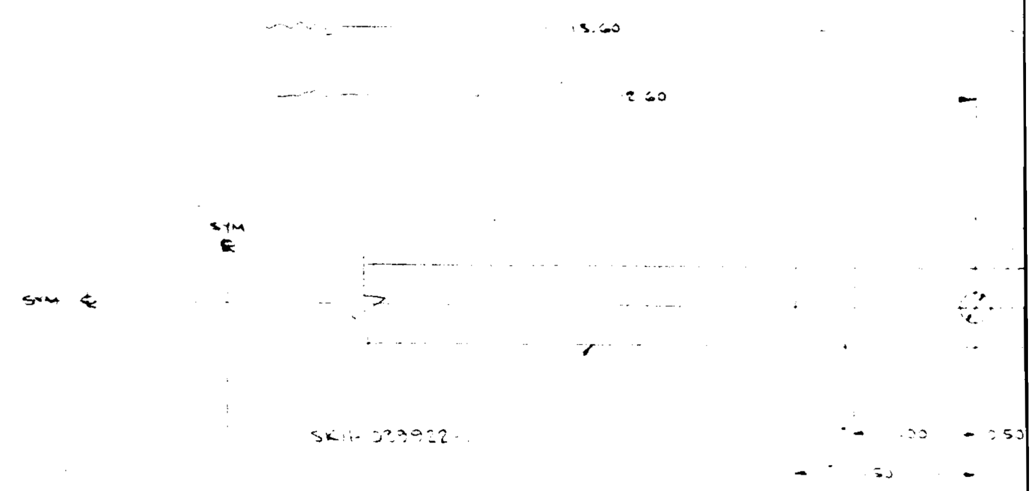

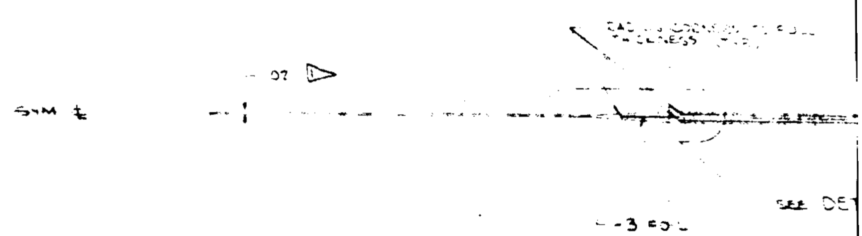

VIEW B-B
(TWICE SIZE)

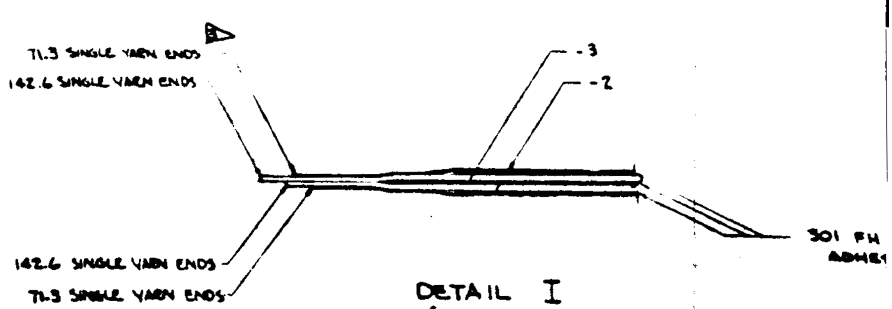

DETAIL I
(NO SCALE)

FIG-1-2

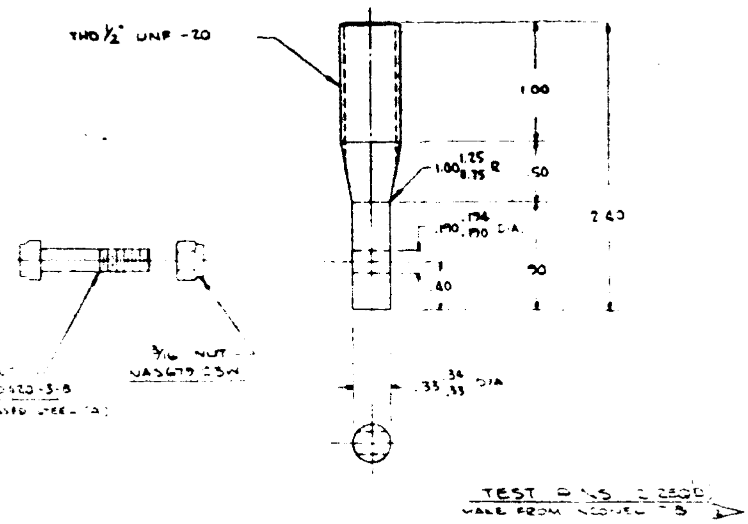

NOTES:

1. PART CONSISTS OF A TOTAL OF 38 STRANDS ... REQUIRES ... WRAPS FROM END TO END ...

2. MATERIALS:
   ROVING - ...
   GLASS - ...
   ADHESIVE - SEE 3

3. RESIN CONTENT:

4. CURE CYCLE:

5. TENSION CONTROL:

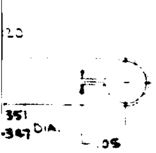

LOCATE SLITS IN FOILS 90° APART. DRILL .190 HOLE 90° FROM SLITS

HYDROBLAST & MEK CLEAN ALL METAL SURFACES. COAT WITH .002 THICK BMS 8-30 (ALUM. FILLED EPOXY-PHENOLIC TYPE I ADHESIVE ON ALL SURFACES OF FOILS & OUTSIDE OF PLUG. AIR DRY ONE HOUR THEN CURE @ 325-350°F FOR 20 MIN. STORE IN POLYETHYLENE BAGS UNTIL USED.

CIRC. WRAPS APPLIED OVER FOIL AREA TO ASSURE ADEQUATE COMPACTION & CONTACT. MAXIMUM THICKNESS = .02 INCH.

HEAT TREAT PER BAC 5616 (TO APPROX. 197 KSI STRENGTH LEVEL)

MATCH DIAMETERS OF -5 & -6 TO PROVIDE A SLIP FIT.

FIGURE 2-3

STRUCTURAL DEVELOPMENT	THE BOEING COMPANY AEROSPACE GROUP SEATTLE WASHINGTON	
D. BARTLETT	FIBERGLASS TENSION ROD LH₂ TANK SUPPORT	
NAS 8-18057	CODE IDENT NO. 81205	SK11-039920
	SCALE NTO	SH 1 OF 1

8

.250 $\frac{.254}{.250}$ DIA HOLE

0.66

-2 FOILS

.093 ▷

DETAIL I

CRES. FOILS - .002 THICK - PER MIL-S-5059
[illegible]IVE COAT PER ▷

NOTES:

1. MATERIALS:
   RESIN - EPON 826 / NMA / BDMA [illegible]
   GLASS - S-994 FIBERGLASS - 12 END ROVING
   ADHESIVE - SEE ▷
2. RESIN CONTENT: 35% ± 2% BY WEIGHT IN FINISHED PART
3. CURE CYCLE: 4 HRS @ 250°F [illegible] 4 HRS @ 300°F
4. TENSION CONTROL: ONLY SLIGHT TENSION SHALL BE APPLIED DURING WINDING TO AVOID FILAMENT DAMAGE. [illegible] BAGGING DURING CURE WILL BE NECESSARY TO OBTAIN ADEQUATE RESIN SQUEEZE OUT.
5. PART CONSISTS OF A TOTAL OF 444 SINGLE-YARN ENDS [illegible] IN FOUR LAYERS AS SHOWN IN DETAIL I.

FIGURE 1-3

▷ PARTS MAY BE WOUND WITH 12 END ROVING AT A RATE OF 9 ROVINGS (108 ENDS) PER INCH PER LAYER.

▷ HYDRO BLAST & MEK CLEAN ALL METAL SURFACES. COAT WITH .002 THICK BMS 8-30 (ALUM FILLED EPOXY-PHENOLIC) TYPE I ADHESIVE ON BOTH SURFACES. AIR DRY ONE HOUR THEN CURE AT 325-350°F FOR 20 MIN. STORE IN POLYETHYLENE BAGS UNTIL USED.

▷ DRAWING TOLERANCES DO NOT APPLY. THICKNESS MAY VARY SLIGHTLY DEPENDING ON MANUFACTURING PROCEDURES

STRUCTURAL DEVELOPMENT	D. BARTLETT 11-8-6	THE BOEING COMPANY AEROSPACE GROUP SEATTLE WASHINGTON	6
	D. BARTLETT 11-8-6	FIBERGLASS TENSION ROD LH2 TANK SUPPORT	
	NAS 8-18037	CODE IDENT NO. 81205 SK11-039922	
		SCALE FULL & NOTED SH 1 OF 1	

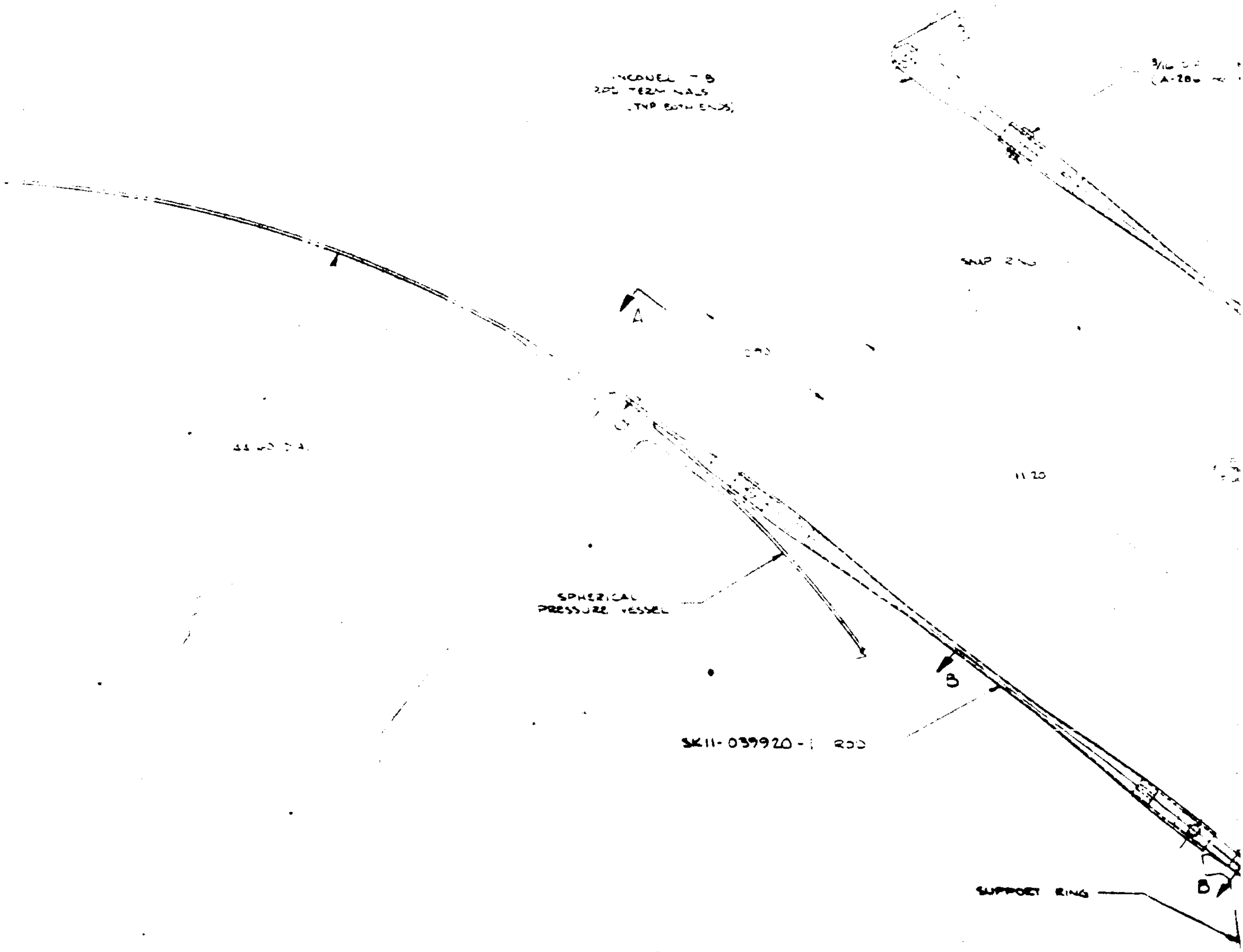

CIRCULAR TENSION ROD
SUPPORT DETAILS
(FULL SIZE)

FIG 2-1

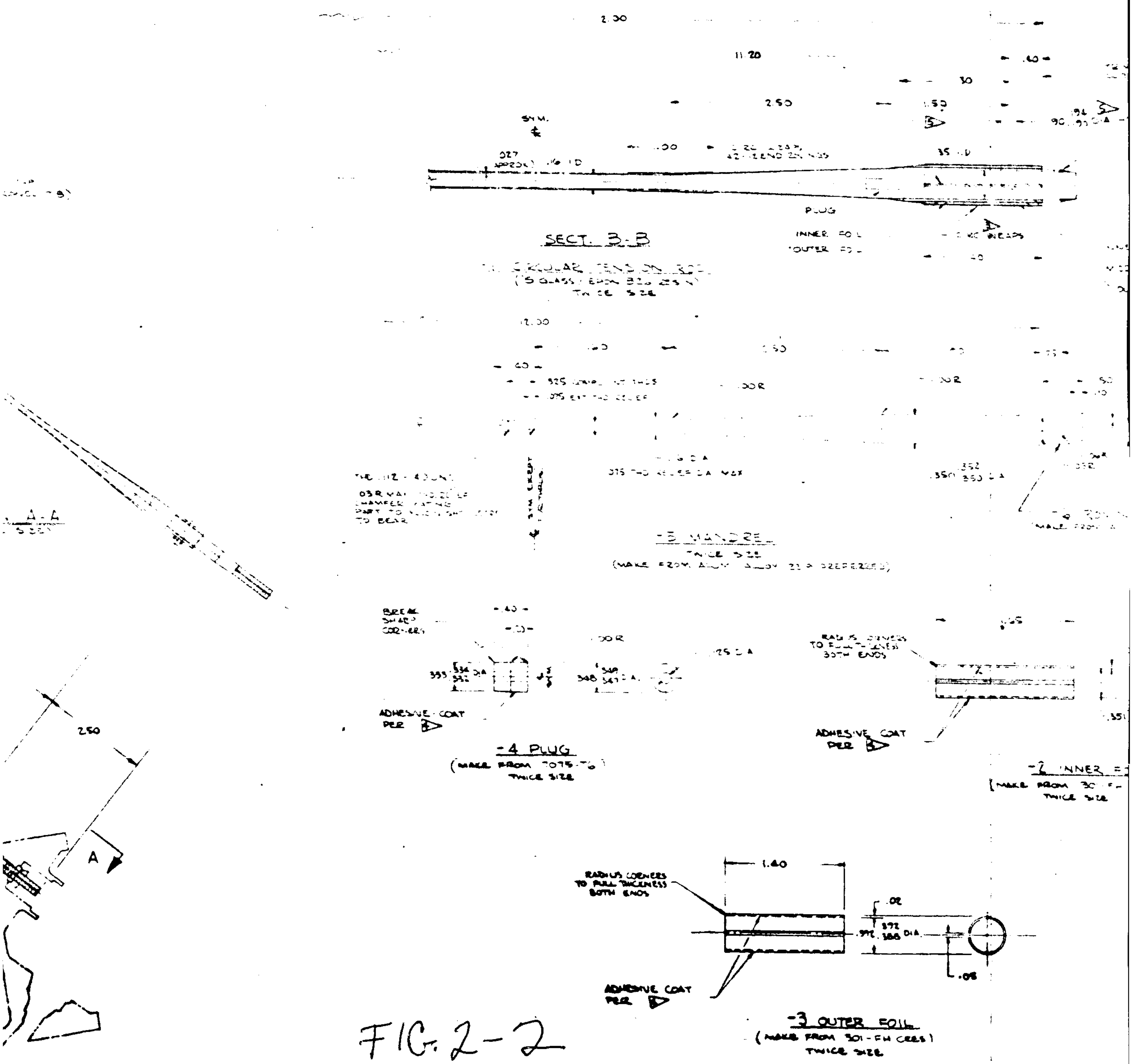
SECT. B-B
PLUG
INNER FOIL
OUTER FOIL
-5 MANDREL
TWICE SIZE
BREAK SHARP CORNERS
ADHESIVE COAT PER
-4 PLUG
(MAKE FROM 7075-T6)
TWICE SIZE
2.50
A
RADIUS CORNERS TO FULL THICKNESS BOTH ENDS
1.40
.02
.08
ADHESIVE COAT PER
-3 OUTER FOIL
(MAKE FROM 301-FH CRES)
TWICE SIZE

FIG. 2-2

action on the adhesive joint caused by yielding and subsequent thickening of foils at the bolt hole. The possibility that this type of yielding could contribute to premature failure is further reason for using a single bolt attachment.

The circular rods must be fabricated on individual mandrels, thus increasing the cost. The mandrel shown on the drawing is assembled by means of a threaded joint which also allows removal after the part is cured. Roving guides on each end of the mandrel are used to position the windings, providing an even distribution over the foil surfaces. The foils are split rings, adhesive coated, and slipped over the windings at the appropriate time. The foils as configured appear expensive since each must be machined from bar stock, however, an alternate design is being considered which uses foils split into two halves. This approach would allow forming the foils from 301 FH stainless steel to a half circle on a brake press, thus reducing machining costs. Circumferential windings are applied over the foil area to provide intimate contact between glass, resin, and adhesive during the cure cycle. The same type of windings are also applied at the small end of the taper section to reduce the tendency for filaments to straighten when loaded. An internal plug is used at the large end of the taper for the same reason. Upon completion of winding, the filaments are cut at the guide, the guide and mandrel halves removed, and the internal plug bonded in place. The mandrel may then be re-used, the only expendable item being the guides. A quantity of these parts may be wound and cured at one time which assures uniform resin content and cure cycle; however, this requires fabrication of a quantity of mandrels. Filament tension control and mandrel tolerances will introduce variables between parts.

A second circular rod design has been developed, however, the design drawing was not available for inclusion in this report. This rod was of the "axe-handle" type, incorporating an internal metallic wedge and an outer metallic ring, with filaments sandwiched between. During the design study it was concluded that the actual wedging action was practically nil and instead the critical feature in design was the adhesive joint strength between filaments and metal. Since in this design only one surface was available for load transfer as opposed to multiple surfaces in the foil joint concept, the diameter of the rod ends was considerably larger than for the foil joints. As a consequence, it was necessary to shorten the fiberglass portion of the rod significantly to avoid interference of the transition joint with the pressure vessel. This particular design was not chosen for the fabrication phase of the program and as a result both circular and flat tension rod designs intended for fabrication and test will incorporate foil joints.

The tentative quantities of tension rods are shown in Table I. The test program requires fabrication of 22 flat and 14 round rods assuming the flat rods are those chosen for LH_2 testing. At present, the feasibility of vibration and impact testing has not been determined. The test plan is to subject the specified quantity of rods to ultimate, cyclic, vibration, and impact loading and then select the best configuration for ultimate and cyclic loading with one end of the rod at -423°F. All parts subjected to limit loading will finally be tested to failure to determine the effects of the particular load environment on ultimate strength.

Compression Struts

The first quarterly report presented a plot (Figure 1) of weight efficiency versus structural index parameter for columnar members of titanium, aluminum, magnesium, and fiberglass. In this report it was pointed out that fiberglass construction offered the least weight in the range of high loads or short columns, and the least heat leak over the entire range of loading considered.

SPECIMEN TYPE	QUANTITY	STATIC	CYCLIC (100 CYCLES MAX)	VIBRATION	IMPACT	LIMIT LOAD	ULTIMATE LOAD	TEMP. AT OPPOSITE ENDS (°F)
TENSION								
. ROUND	5	X					X	R.T. & -320
. FLAT	5	X					X	R.T. & -320
. ROUND	3		X			X		R.T. & -320
. FLAT	3		X			X		R.T. & -320
. ROUND	3			X		X		R.T. & -320
. FLAT	3			X		X		R.T. & -320
. ROUND	3				X	X		R.T. & -320
. FLAT	3				X	X		R.T. & -320
. ROUND OR FLAT	3		X			X		R.T. & -423
. ROUND OR FLAT	5	X					X	R.T. & -423
TOTAL	36							

TABLE 1

It was intended to fabricate struts designed for this high load range for the experimental portion of the program.

During the fifth month Boeing was informed of an interest in using fiberglass compression struts to support LH_2 tanks for a MSFC launch experiment. It was suggested that the experimental data from this contract might be of more value if compression struts configured to meet the geometry and load requirements of this particular launch stage were fabricated and tested. To meet the more stringent deadline, the work on compression struts has been accelerated to provide final test data by March 1, 1967.

Figure 3 is the design drawing of the compression strut selected for fabrication and test. The part is designed for an ultimate compressive or tensile load of 4000 lbs, and would be expected to fail in compression by buckling or crushing. Spherical bearings have been provided at each end to allow for misalignment of attachment points. The part has been designed to allow a maximum of .05 inches eccentricity between pinned ends, which is believed adequate to account for warpage and tolerance build up caused by the end fittings. It is planned to wet wind the parts with an Epon 826 resin system and 12 end S-994 glass roving on an aluminum mandrel. The cured part will then be slipped from the mandrel, trimmed and bonded to end fittings with Narmco 7343 adhesive. Materials for these parts have been ordered and tool design has been started.

Table 2 shows the tentative quantities of test parts and the types of testing planned. The possibility of conducting meaningful vibration tests has not been explored thoroughly and such testing may be eliminated from the program. Cyclic load specimens will be tested to failure upon successful completion of cyclic tests to reveal any detrimental effects.

13 12 11 10 9

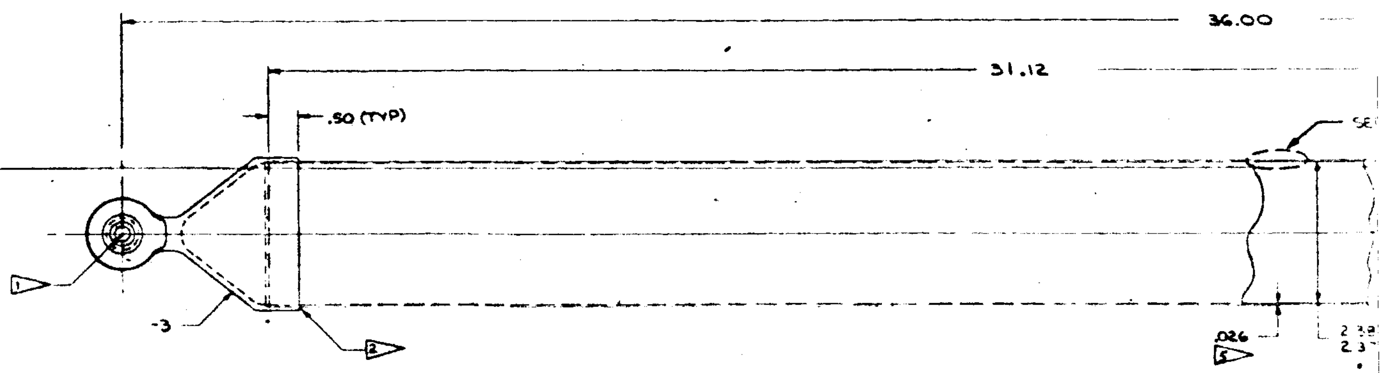

FIG-3-1

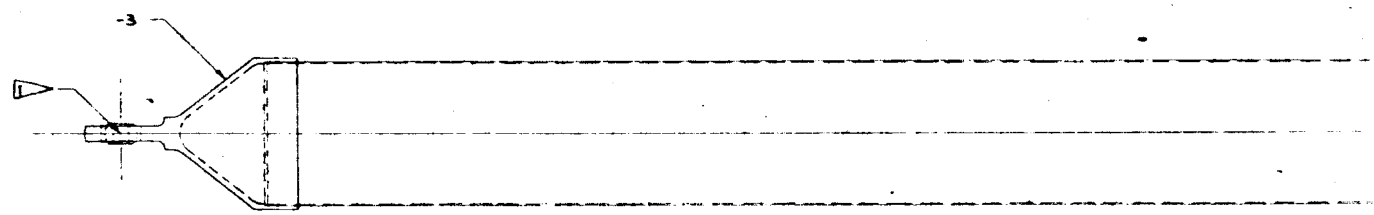

-1 SUPPORT TU

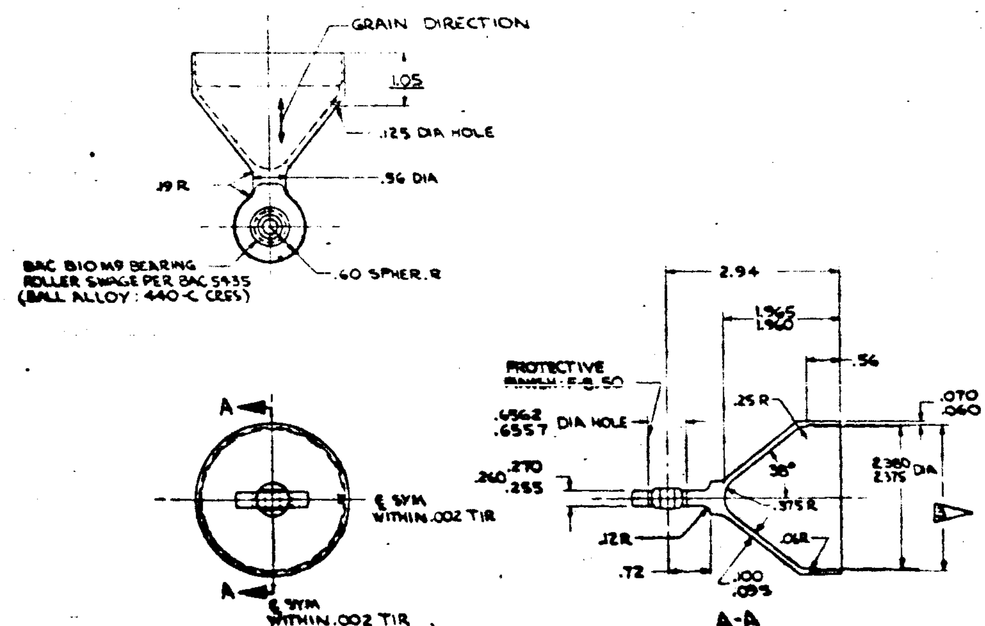

-3 FITTING DETAIL
SCALE: 1/1

8	7	6	5	4

125/ALL MAC

1 BEARI

2 BONC APP HYD FIB

3 THIS OF AI

4 MATE

5 DRAW TH PRO

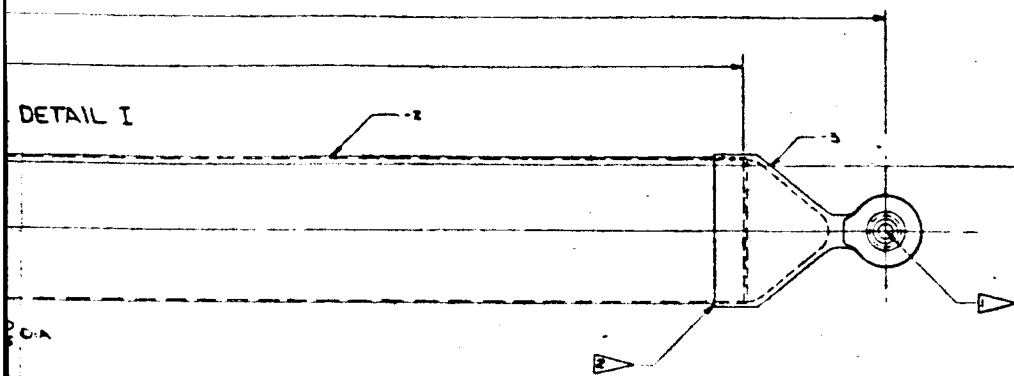

FIG 3-2

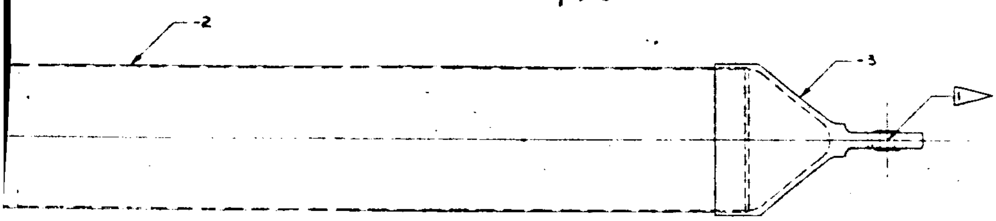

JBE ASSY

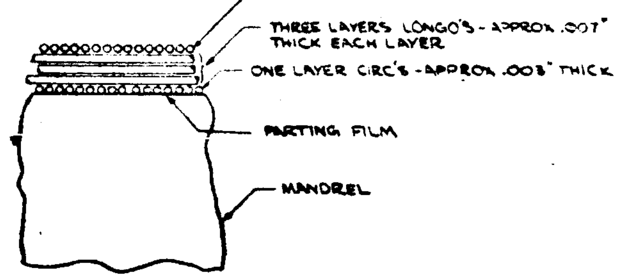

DETAIL I
NO SCALE

BASIC RIVET CODE	

NEXT ASSY	USED ON		SERIAL NUMBER	PART NUMBER			REV LTR

APPLICATION

8	7	6	5	4

REVISIONS

ZONE	LTR	DESCRIPTION	DATE	APPROVED

HINED SURFACES

IG CENTERLINES (AT OPPOSITE ENDS) SHALL BE CONCENTRIC WITHIN .05 TIR.

-3 TO -2 USING NARMCO 7343/7139 POLYURETHANE (11PHR) ADHESIVE.
LY 5 MIL COATING ON FAYING SURFACES. CURE 4 HRS @ RT AND 2 HRS. @ 180°F.
ROBLAST & CHEM. CLEAN METAL SURFACES PER BAC 5765. MEK CLEAN
ERGLASS SURFACES ONLY.

DIAMETER TO MATCH O.D. OF -2 AFTER APPLICATION OF .003"
DHESIVE ON MATING SURFACES.

RIAL: FIBERGLASS: S-944 SINGLE END AND 12 END ROVING.
RESIN SYSTEM: EPON 826, MNA, BDMA (100:90:1.5). RESIN
CONTENT TO BE 18% ± 2% BY WEIGHT.
CURE CYCLE: 4 HOURS @ 250°F, POST CURE: 2 HOURS @ 300°F

ING TOLERANCES DO NOT APPLY.
CKNESS MAY VARY SLIGHTLY DEPENDING ON MANUFACTURING
OCEDURES

FIGURE 3-3

LIST OF MATERIAL

	QTY REQD	PART OR IDENTIFYING NUMBER	NOMENCLATURE OR DESCRIPTION	ZONE	MATERIAL AND SPECIFICATION	HT TR	FINISH	PT. NO	REV LTR
✓	2	BACB10 M9	BEARING-PLAIN SPHER.		440C CRES BALL				
✓	2	-3	FITTING		2.60 × 2.60 × 3.50 2024-T62 AL PLATE PER QQ-A-250/4 (NOTE GRAIN DIRECTION)		F-650 IN AREAS NOTED	R	
✓	1	-2	TUBE		4			R	
–	–	-1	SUPPORT TUBE ASSY					R	
-1									

RELEASE

CONTRACT NAS 8-8037

DR Dan Good

STRUCT

L. BARTLETT

THE BOEING COMPANY
AERO-SPACE DIVISION SEATTLE, WASHINGTON

SUPPORT TUBE ASSY
(TEST ONLY)

SIZE J CODE IDENT NO 81205 SK11-039921

SCALE FULL SH OF 1

SK11-039921

LOAD	QUANTITY	STATIC	CYCLIC (100 CYCLES MAX)	VIBRATION	LIMIT LOAD	ULTIMATE LOAD	TEMP. AT OPPOSITE ENDS (°F)
COMPRESSION	1	X				X	R.T. & R.T.
	2	X				X	R.T. & -320
	1			X	X		R.T. & -320
TENSION	1	X				X	R.T. & -320
COMPRESSION AND TENSION	2		X		X		R.T. & -320

TOTAL 7

TABLE 2

Beams

Beam designs have not been developed sufficiently to warrant discussion in this section. Instead a discussion of initial computer program results has been included in Section 3.0, "Analytical Approach".

3.0 ANALYTICAL APPROACH

Tension Rods

Design of flat tension rods constitutes a trade between bolt diameter, rod width, quantity of foils, and foil gage. Due to the manufacturing techniques employed, the rod width is the same for the entire length of the part. This is believed advantageous since each filament is able to transfer load from end to end without depending entirely on resin shear strength as in the case of a tensile rod machined to a reduced width in the central portion. High strength bolts of 3/16 and 1/4 inch diameter, used in shear, appeared suitable for the design ultimate load of 4000 lbs. It was assumed that the filaments transferred load to the foils through adhesive bond within a one inch lap length and that each foil, regardless of the quantity, carried a proportional share of the total load. Figure 4 is an illustration of the various parameters considered in selecting a specimen for fabrication and test. The shaded area on both plots indicates inadequate design and the three dark vertical lines indicate some available gages of 301 stainless steel. The "bearing" curve was constructed using the criteria that yield strength of the foil material would not be exceeded at ultimate load. In all cases it was assumed that bearing strength of the bolt was equivalent to the foil material. The "tension" curve is based on net section tension stress at the bolt. From these curves it can be seen that if a 3/16 inch bolt is selected either four .020 gage foils or three .025 gage foils are necessary. For a 1/4 inch bolt, it is possible to use three .020 gage foils. Since three foils simplify the assembly job, and .020 gage provides the minimum thickness, the 1/4 inch bolt size was selected.

Room temperature properties were used in design of all tension rods since one end will be external to the insulation on a cryogenic tank. The literature has shown that an increase in strength level accompanies a reduction in temperature for the materials used, therefore, the weakest part of the structure is

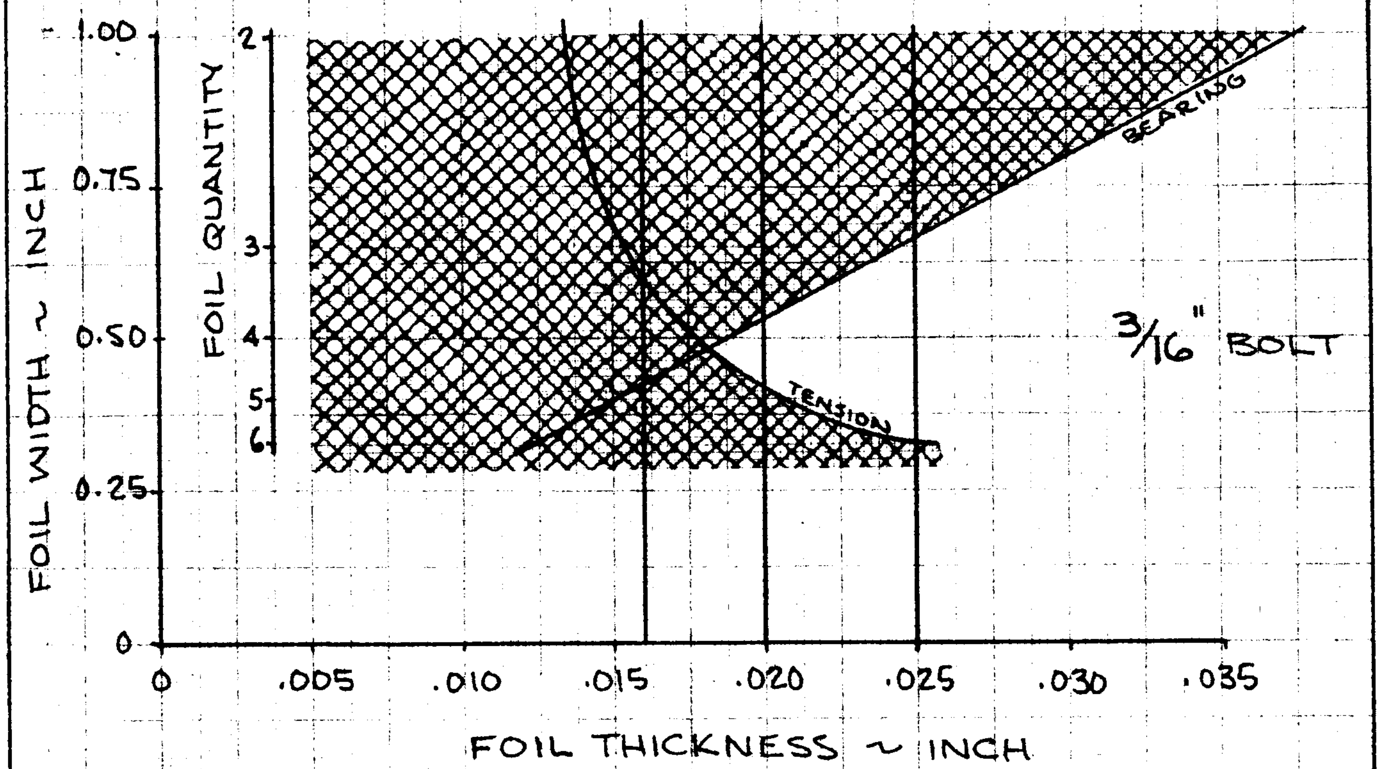

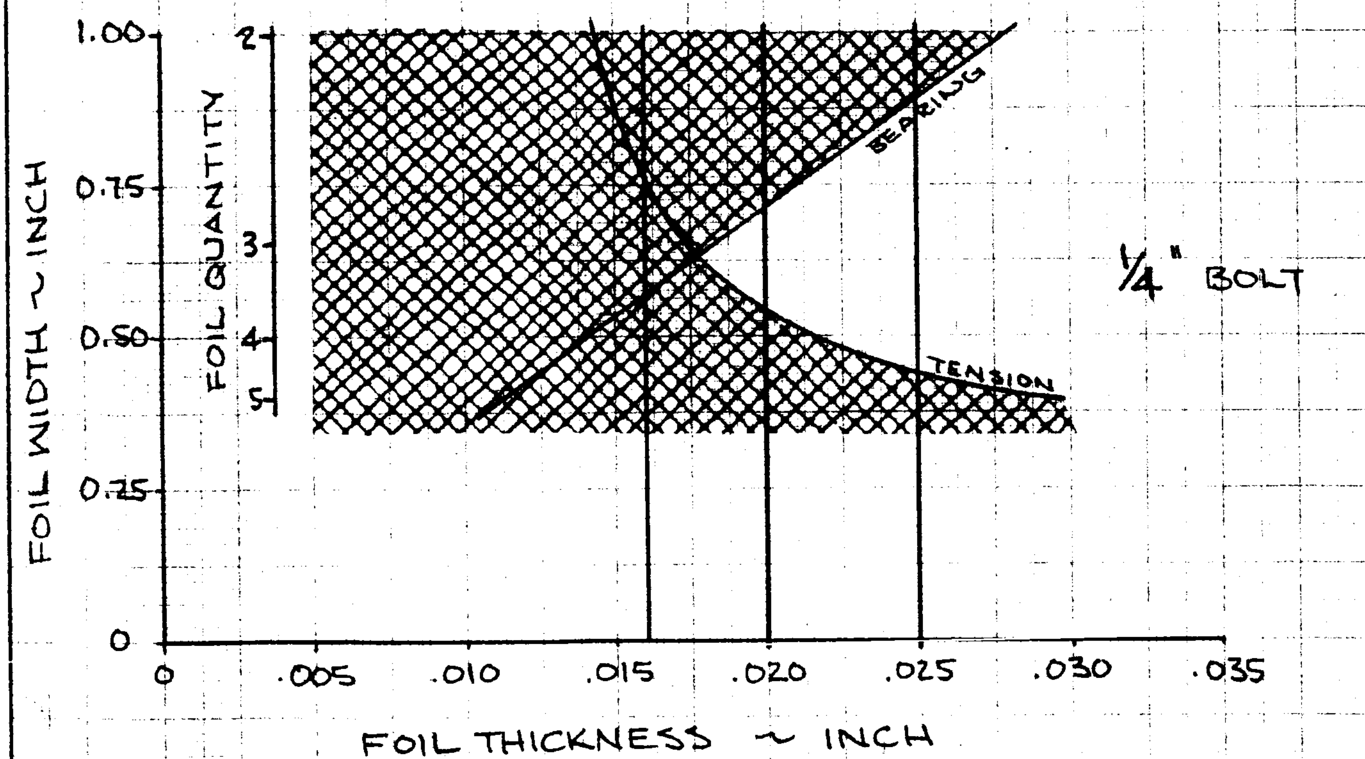

	INITIALS	DATE	REV BY INITIALS	DATE	TITLE	MODEL
CALC					FLAT TENSION ROD DESIGN PARAMETERS	
CHECK						
APPD.						
APPD.						

U3 4013 8000 REV. 12-64

REV LTR______

BOEING NO FIGURE 4

SH

at the warm end. The foil widths of Figure 4 were established using an allowable "pull out" load of 2020 lb/inch of foil width. An allowable ultimate glass stress of 450,000 psi and a resin content of 31.6% by volume were used in design.

The design of the circular tension rod employs an internal attachment lug to minimize the diameter of the end attachments. A 3/16 inch shear pin was selected since smaller diameters would result in excessive bearing stress in the foils. A larger pin was not practical since there would be insufficient net section area in the attachment lug. The same assumptions that were made for flat tension rods regarding load capacity of the bonded joints were also used for the round tension rods. The circumferential windings at the small end of the taper section were sized to limit radial extension at ultimate load to 0.1% . The allowable ultimate glass stress and resin content used for the flat rods was also used for circular rods.

Compression Struts

The fiberglass and titanium struts were designed as imperfect columns with an initial imperfection (displacement) of .05 inches. The columns were optimized by equating the eccentrically loaded column extreme fiber stress to the tube wall local crushing stress, solving for the optimum wall thickness and diameter using a trial and error routine program with the aid of a digital computer. The governing equations are:

Tube Wall Local Crushing Stress

$$(1) \quad F_{cc} = .25\ E\ t/R$$

Maximum Fiber Stress of a Slightly Bent Column

$$(2) \quad F_c = P/A + \frac{P\ y_1\ R}{(1-P/P_e)\ I} = P/A \left\{ 1.0 + \frac{2\ y_1}{(1-\lambda)\ R} \right.$$

P = Column load

A = Column area

y_1 = Initial imperfection (displacement)

P_e = Euler buckling load = $\frac{\pi^2 EI}{L^2}$

λ = P/P_e

R = median tube radius

Designing the struts as imperfect columns increased the area of the fiberglass struts by approximately 19% and the titanium strut by 25%. The eccentricity is not as detrimental to the fiberglass strut as the titanium strut because the optimum diameter is larger and the eccentricity therefore causes less outer fiber stress.

An illustration of the effect of strut material and eccentricity on heat flow is shown in Figure 5. The figure shows that the fiberglass strut has approximately 70% less heat flow than a titanium strut. Titanium alloy was used for this comparison since it has the lowest thermal conductivity of the more common metals. The effect of eccentricity adds only slight heat flow to the fiberglass part whereas a significant addition occurs with titanium. The single curve shown in the figure represents an optimization on fiberglass strut heat flow, the lowest point occurring at about 2.4 inches in diameter. If a particular design application requires a smaller diameter strut, the curve shows the accompanying heat flow penalties. The entire optimization curve was not produced for the titanium parts or the fiberglass part with zero eccentricity, but the points shown represent the lowest (optimum) heat flow attainable.

Beams

The description of the digital computer program that was written to determine the optimum beam geometry for the aluminum and fiberglass beams was described in monthly progress report number 3.

The initial beam concept resulting from a preliminary trade study of various methods of construction (reported in quarterly progress report number 1) is shown in Figure 6. Initial computer runs with this concept indicated

COLUMN LENGTH BETWEEN CENTERS = 36 INCH
COLUMN LOAD = ± 4000 LB (ULTIMATE)

FIBERGLASS STRUT:
S-994 GLASS, E-787 RESIN BFW.
$E = 5 \times 10^6$ psi. $K = .025 \frac{\text{BTU-IN}}{\text{IN}^2\text{-HR-}^\circ\text{F}}$

TITANIUM STRUT:
6AL-4V ALLOY
$E = 16 \times 10^6$ psi $K = 0.24 \frac{\text{BTU-IN}}{\text{IN}^2\text{-HR-}^\circ\text{F}}$

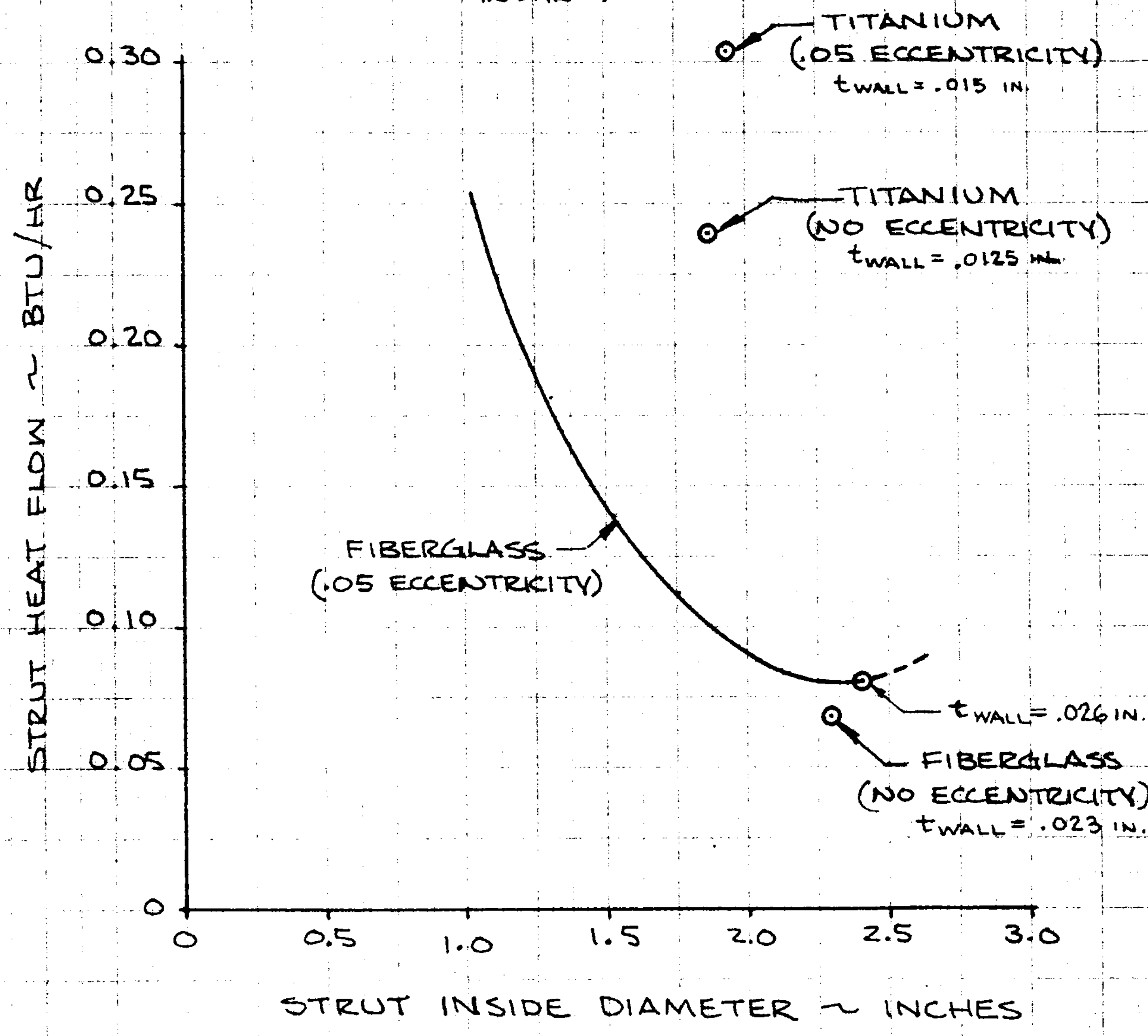

	INITIALS	DATE	REV BY INITIALS	DATE	TITLE	MODEL
CALC					EFFECT OF STRUT MATERIAL AND DIAMETER ON HEAT FLOW	
CHECK						
APPD.						
APPD.						

U3 4013 8000 REV. 12-64

REV LTR

BOEING NO FIGURE 5

SH

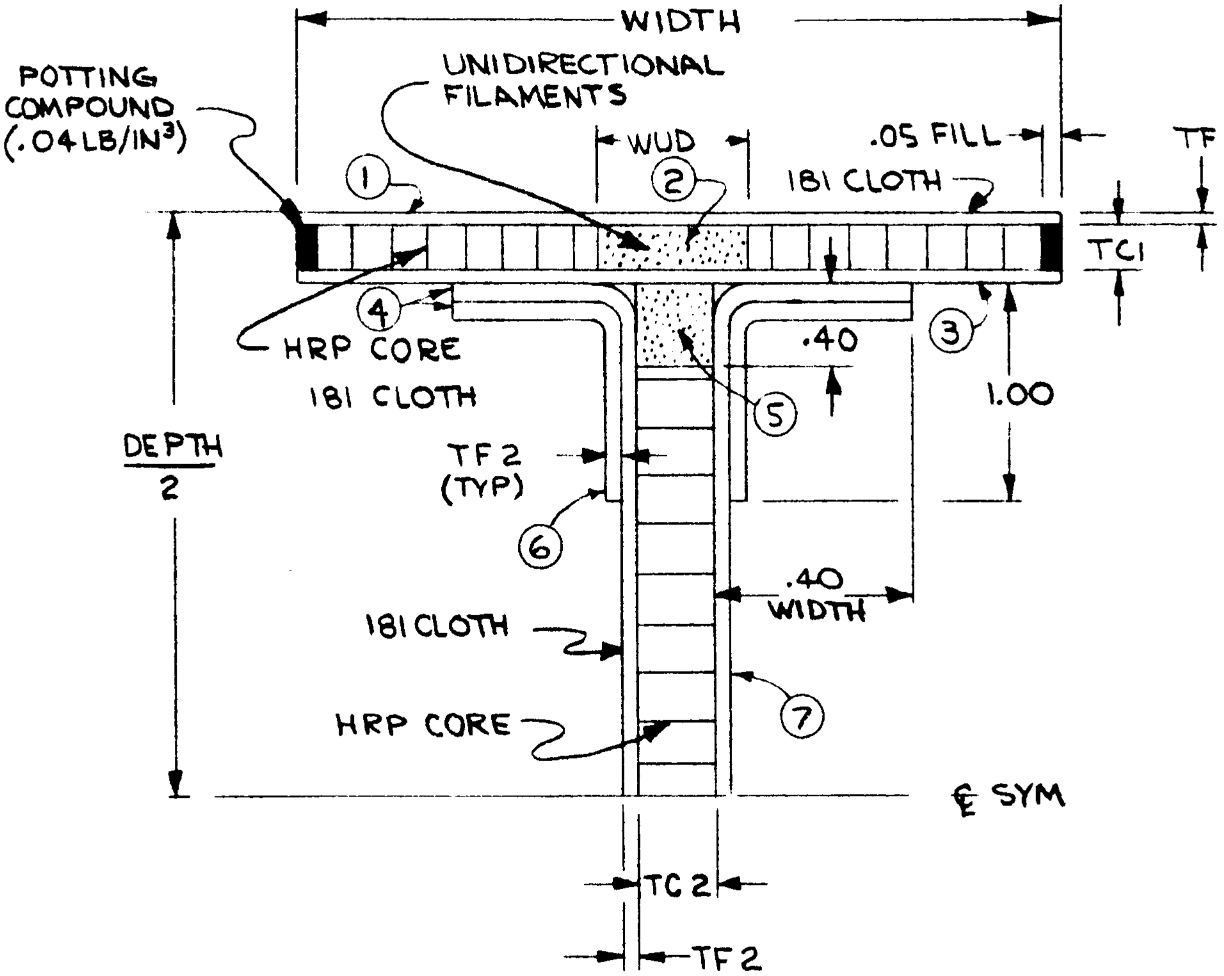

INITIAL CONCEPT

FIGURE 6

improved efficiency if element #5 was eliminated entirely. For example, in the case of low load beams there were sufficient unidirectional fibers in element #5 and element #2 was not needed. However, when element #2 was removed it became necessary to increase the thickness of elements #1 and #3 for lateral stability requirements. Conversely, if element #5 were eliminated load could be carried with element #2 and lateral stability of the section was improved. The higher loaded beams with greater depth required increased thickness of the web core TC2 to prevent web instability, which automatically increased the width of element #5. Element #5 then frequently became critical in shear along the facing of elements #7 for this increased thickness. This is because there is a definite maximum thickness of unidirectional filaments permitted in order to be able to work the filaments to their ultimate axial strength level and yet not exceed the adhesive shear allowable along the faces. It is interesting to note that changing the dimension normal to the thickness direction has no beneficial effect on load transfer by adhesive shear for an optimum beam.

The final beam concept is shown in Figure 7. The entire beam digital computer program was run with this concept for both fiberglass and 7178-T6 aluminum construction. The aluminum beam was run using exactly the same construction as the fiberglass beam. The fiberglass honeycomb core HRP-3/16 4.0 was replaced by aluminum honeycomb core 5052-3/16 4.4. All other elements were 7178-T6 aluminum sheet. An adhesive shear allowable of 1600 lbs/in^2 was used for the fiberglass beam. Since the aluminum beam could employ rivets in addition to bonding, the expression for adhesive shear in the program was increased to 2500 lbs/in^2.

Figures 8, 9, 10, and 11 show case summaries of the computer runs.

A tally of the mode of failure which resulted in the minimum allowable beam

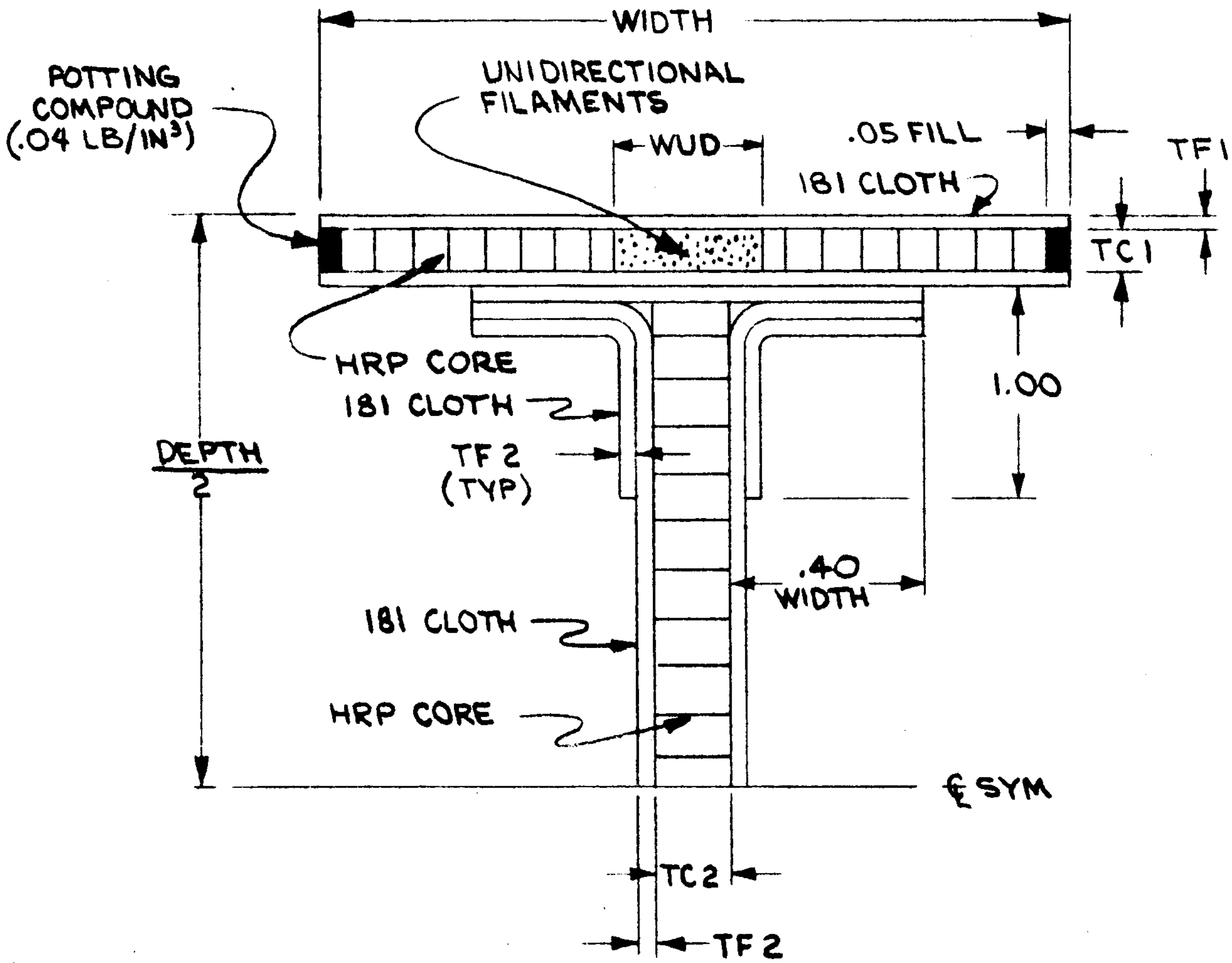

FINAL CONCEPT

FIGURE 7

	FIBERGLASS		ALUMINUM
VARIABLES		**VARIABLES**	
SPAN	20"	SPAN	20"
DEPTH	4,5,6,7,8,9,10,11,14,16,20,24	DEPTH	4,6,8,10,12,14,16
TC2	.10, .25, .375	TC2	.10, .25, .375, .50
TF2	.009,.018,.027,.036, .054	TF2	.009,.018,.027,.036
WUD	.25,.50,1.0,1.5,2.0	WUD	.25,.50,1.0,1.5,2.0
WIDTH	2.0 (1)	WIDTH	2.0 (1)
TC1	.081 (2)	TC1	.081
TF1	.009,.018,.027,.036	TF1	.009,.018,.027,.036

MODE OF FAILURE	NO. OF CASES CRITICAL	MODE OF FAILURE	NO. OF CASES CRITICAL
1. MAX. ALLOWABLE STRAIN	0	1. MAX. ALLOWABLE STRAIN	0
2. ADHESIVE SHEAR 1-2	(FSU=1600 P.S.I.) 0	2. ADHESIVE SHEAR 1-2	(FSU=2500 P.S.I.) 0
3. ADHESIVE SHEAR 2-3	" 280	3. ADHESIVE SHEAR 2-3	" 3
4. DELETED = 26,000 #	22	4. DELETED = 26,000 #	144
5. DELETED	0	5. DELETED	0
6. ULT SHEAR ~ WEB FACING	0	6. ULT SHEAR ~ WEB FACING	0
7. WEB BUCKLING SHEAR + COMP. + BENDING	1093	7. WEB BUCKLING SHEAR + COMP. + BENDING	675
8. WEB INTRACELL BUCKLING	1071	8. WEB INTRACELL BUCKLING	1384
9. WEB FACE WRINKLING	509	9. WEB FACE WRINKLING	34
10. FLANGE INTRACELL BUCKLING	289	10. FLANGE INTRACELL BUCKLING	0
11. FLANGE FACE WRINKLING	0	11. FLANGE FACE WRINKLING	0
12. FLANGE SHEAR CRIMPING	0	12. FLANGE SHEAR CRIMPING	0
13. FLANGE CRIPPLING	16	13. FLANGE CRIPPLING	0
14. FLANGE LATERAL STABILITY	0	14. FLANGE LATERAL STABILITY	0
TOTAL CASES	3280	TOTAL CASES	2240
UNIVAC 1108 COMPUTER TIME	5 MIN. 26 SEC.	UNIVAC 1108 COMPUTER TIME	2 MIN. 19 SEC.

(1) LARGER WIDTH NEVER REQUIRED FOR 20" SPAN ~ REF. MODE 14

(2) MAX. THICKNESS ALLOWED FOR ADHESIVE SHEAR CRITICAL MODE 3

	INITIALS	DATE	REV BY INITIALS	DATE	TITLE	MODEL
CALC					BEAM OPTIMIZATION STUDY CASE SUMMARY SPAN = 20 INCHES	
CHECK						
APPD						
APPD						

FIBERGLASS		ALUMINUM	
VARIABLES		**VARIABLES**	
SPAN	40"	SPAN	40"
DEPTH	4,6,8,10,12,16,20,24	DEPTH	4,6,8,10,12,16,20,24
TC2	.10, .25, .375, .50	TC2	.10, .25, .375, .50
TF2	.009, .018, .027, .036, .054	TF2	.018, .027, .036, .045
WUD	.25, .50, 1.0, 1.5, 2.0	WUD	.25, .50, 1.5, 2.0
WIDTH	2, 3	WIDTH	2, 3
TC1	.081, .163 [1]	TC1	.081, .163
TF1	.009, .018, .027, .036	TF1	.009, .018, .027, .036

MODE OF FAILURE	NO. OF CASES CRITICAL	MODE OF FAILURE	NO. OF CASES CRITICAL
1. MAX. ALLOWABLE STRAIN	0	1. MAX. ALLOWABLE STRAIN	0
2. ADHESIVE SHEAR 1-2	(FSU = 1600 P.S.I) 0	2. ADHESIVE SHEAR 1-2	(FSU = 2500 P.S.I) 0
3. ADHESIVE SHEAR 2-3	" 230	3. ADHESIVE SHEAR 2-3	" 23
4. DELETED = 26,000 #	41	4. DELETED = 26,000 #	1500
5. DELETED	0	5. DELETED	0
6. ULT SHEAR ~ WEB FACING	0	6. ULT SHEAR ~ WEB FACING	0
7. WEB BUCKLING SHEAR + COMP. + BENDING	2241	7. WEB BUCKLING SHEAR + COMP. + BENDING	1318
8. WEB INTRACELL BUCKLING	1763	8. WEB INTRACELL BUCKLING	2810
9. WEB FACE WRINKLING	481	9. WEB FACE WRINKLING	186
10. FLANGE INTRACELL BUCKLING	305	10. FLANGE INTRACELL BUCKLING	145
11. FLANGE FACE WRINKLING	0	11. FLANGE FACE WRINKLING	0
12. FLANGE SHEAR CRIMPING	0	12. FLANGE SHEAR CRIMPING	0
13. FLANGE CRIPPLING	1138	13. FLANGE CRIPPLING	274
14. FLANGE LATERAL STABILITY	1252	14. FLANGE LATERAL STABILITY	144
TOTAL CASES	7424	TOTAL CASES	6400
UNIVAC 1108 COMPUTER TIME	10 MIN. 1 SEC.	UNIVAC 1108 COMPUTER TIME	6 MIN. 38 SEC.

[1] MAX. THICKNESS ALLOWED FOR ADHESIVE SHEAR CRITICAL MODE 3

	INITIALS	DATE	REV BY INITIALS	DATE	TITLE	MODEL
CALC					BEAM OPTIMIZATION STUDY	
CHECK					CASE SUMMARY	
APPD					SPAN = 40 INCHES	
APPD						

FIBERGLASS		ALUMINUM	
VARIABLES		**VARIABLES**	
SPAN	60"	SPAN	60"
DEPTH	6, 8, 10, 12, 16, 20, 24	DEPTH	4, 8, 14, 20, 24
TC2	.10, .25, .375, .50	TC2	.10, .25, .375, .50
TF2	.018, .027, .036, .045, .054	TF2	.009, .018, .027, .036
WUD	.50, 1.0, 1.5, 2.0	WUD	.25, .50, 2.0
WIDTH	2, 3, 4	WIDTH	2, 3, 4
TC1	.081, .163, .244 [1]	TC1	.081, .163, .244, .325
TF1	.009, .018, .027, .036	TF1	.009, .018, .027, .036

MODE OF FAILURE	NO. OF CASES CRITICAL	MODE OF FAILURE	NO. OF CASES CRITICAL
1. MAX. ALLOWABLE STRAIN	0	1. MAX. ALLOWABLE STRAIN	0
2. ADHESIVE SHEAR 1-2	(FSU = 1600 P.S.I.) 0	2. ADHESIVE SHEAR 1-2	(FSU = 2500 P.S.I.) 0
3. ADHESIVE SHEAR 2-3	" 32	3. ADHESIVE SHEAR 2-3	" 45
4. DELETED = 26,000 #	77	4. DELETED = 26,000 #	1304
5. DELETED	0	5. DELETED	0
6. ULT SHEAR ~ WEB FACING	0	6. ULT SHEAR ~ WEB FACING	0
7. WEB BUCKLING SHEAR + COMP. + BENDING	3457	7. WEB BUCKLING SHEAR + COMP. + BENDING	3899
8. WEB INTRACELL BUCKLING	1121	8. WEB INTRACELL BUCKLING	3706
9. WEB FACE WRINKLING	448	9. WEB FACE WRINKLING	133
10. FLANGE INTRACELL BUCKLING	316	10. FLANGE INTRACELL BUCKLING	230
11. FLANGE FACE WRINKLING	0	11. FLANGE FACE WRINKLING	0
12. FLANGE SHEAR CRIMPING	0	12. FLANGE SHEAR CRIMPING	0
13. FLANGE CRIPPLING	2908	13. FLANGE CRIPPLING	750
14. FLANGE LATERAL STABILITY	5105	14. FLANGE LATERAL STABILITY	1453
TOTAL CASES	13,464	TOTAL CASES	11,520
UNIVAC 1108 COMPUTER TIME	24 MIN. 11 SEC.	UNIVAC 1108 COMPUTER TIME	13 MIN. 25 SEC.

[1] MAX THICKNESS ALLOWED FOR ADHESIVE SHEAR CRITICAL MODE 3

	INITIALS	DATE	REV BY INITIALS	DATE	TITLE	MODEL
CALC					BEAM OPTIMIZATION STUDY CASE SUMMARY SPAN = 60"	
CHECK						
APPD						
APPD						

FIBERGLASS	
VARIABLES	
SPAN	80"
DEPTH	8, 10, 13, 16, 20, 24
TC2	.10, .25, .375, .50
TF2	.009, .018, .027, .036, .054
WUD	.50, 1.5, 2.0
WIDTH	2, 3, 4
TC1	.081, .163, .244, .325
TF1	.009, .018, .027, .036

MODE OF FAILURE		NO. OF CASES CRITICAL
1. MAX. ALLOWABLE STRAIN		0
2. ADHESIVE SHEAR ①-②	(FSU = 1600 P.S.I.)	0
3. ADHESIVE SHEAR ②-③	"	0
4. DELETED = 26,000 #		9
5. DELETED		0
6. ULT SHEAR ~ WEB FACING		0
7. WEB BUCKLING SHEAR + COMP. + BENDING		3064
8. WEB INTRACELL BUCKLING		1323
9. WEB FACE WRINKLING		3
10. FLANGE INTRACELL BUCKLING		0
11. FLANGE FACE WRINKLING		0
12. FLANGE SHEAR CRIMPING		0
13. FLANGE CRIPPLING		942
14. FLANGE LATERAL STABILITY		5819
TOTAL CASES		11,160
UNIVAC 1108 COMPUTER TIME		23 MIN.

ALUMINUM	
VARIABLES	
SPAN	80"
DEPTH	4, 8, 14, 20, 24
TC2	.10, .25, .375, .50
TF2	.009, .018, .027, .036
WUD	.25, .50, 2.0
WIDTH	2, 3, 4
TC1	.081, .163, .244, .325
TF1	.009, .018, .027, .036

MODE OF FAILURE		NO. OF CASES CRITICAL
1. MAX. ALLOWABLE STRAIN		0
2. ADHESIVE SHEAR ①-②	(FSU = 2500 P.S.I.)	0
3. ADHESIVE SHEAR ②-③	"	0
4. DELETED = 26,000 #		800
5. DELETED		0
6. ULT SHEAR ~ WEB FACING		0
7. WEB BUCKLING SHEAR + COMP. + BENDING		3416
8. WEB INTRACELL BUCKLING		2565
9. WEB FACE WRINKLING		72
10. FLANGE INTRACELL BUCKLING		130
11. FLANGE FACE WRINKLING		0
12. FLANGE SHEAR CRIMPING		0
13. FLANGE CRIPPLING		987
14. FLANGE LATERAL STABILITY		3550
TOTAL CASES		11,520
UNIVAC 1108 COMPUTER TIME		13 MIN. 26 SEC.

	INITIALS	DATE	REV BY INITIALS	DATE	TITLE	MODEL
CALC					BEAM OPTIMIZATION STUDY CASE SUMMARY SPAN = 80"	
CHECK						
APPD						
APPD						

load was recorded for each case. The tabulation shows that several of the modes of failure were never critical for any of the combinations of variables run. Future investigations could eliminate these failure modes and reduce computer time. Referring to Figures 8, 9, 10, and 11, the failure modes that could be eliminated are:

1. Max allowable strain
2. Adhesive shear - element #1 to #2
4. This mode of failure was deleted when beam element #5 was eliminated. It was arbitrarily set = 26,000 lbs. Therefore cases appearing in this mode mean that all other modes of failure were greater than 26,000 lbs. This gives an indication that the range of geometry variables were large enough to cover the range of loading under investigation.
5. This mode of failure was deleted when beam element #5 was eliminated.
11. Flange face wrinkling.
12. Flange shear crimping due to compression loading.

The results of the computer program showing beam efficiency (beam load divided by beam weight) for the different spans and material are shown on Figures 12 through 19. Beam depths have been recorded at each plotted point. Maximum beam depths of 24" were run for all cases but were never efficient. It is shown that optimum beam depth is difficult to determine because the depth can be varied without much change in weight, however, a trend can be seen. A 10% weight increase line has been added to these curves to show the large range of beam depths possible with nominal weight penalty. This information could be of value in designing beams where available space limits the depth.

Figure 20 shows the final weight comparison as a result of the computer program. It can be seen that the fiberglass construction offers some weight

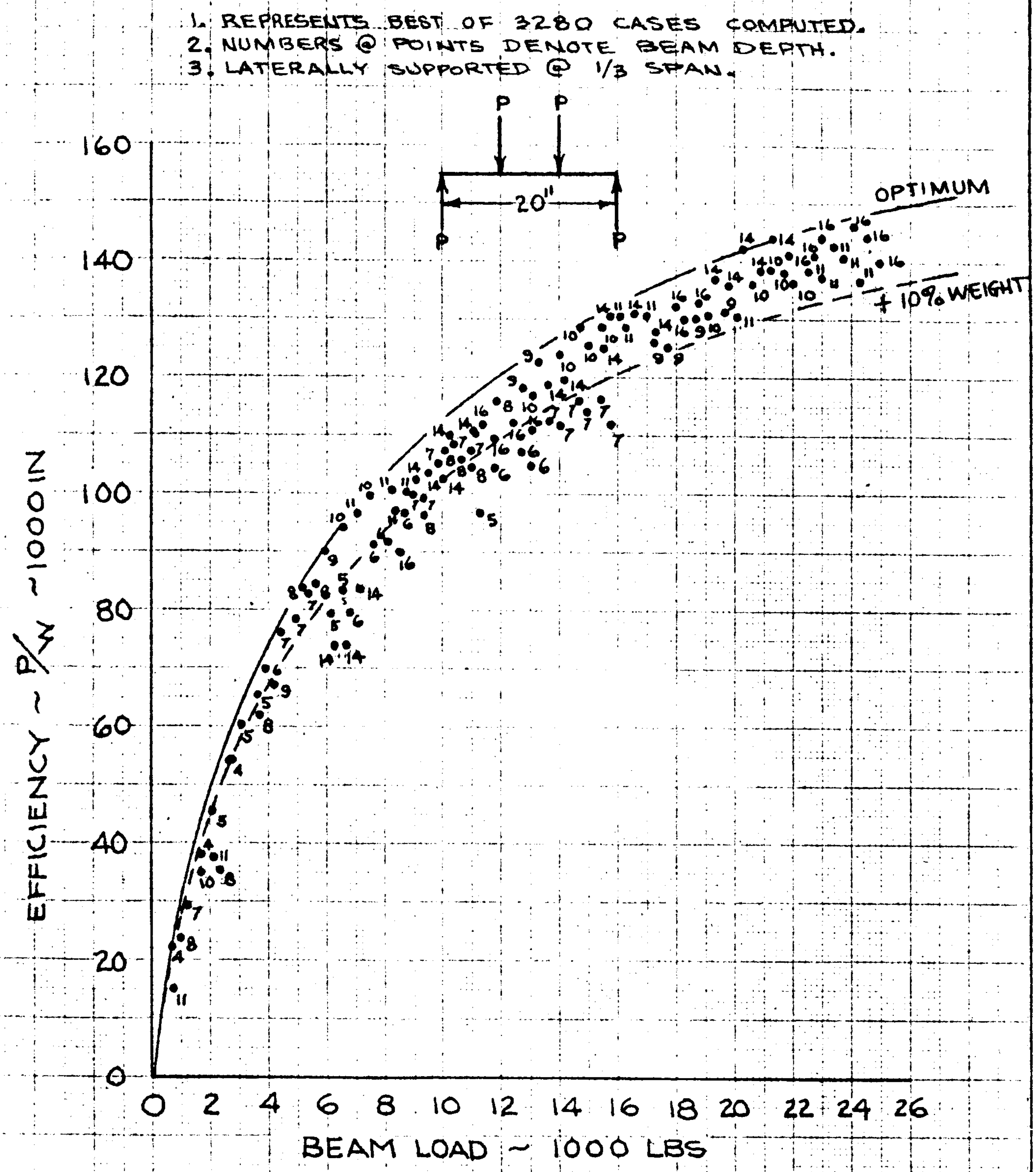

	INITIALS	DATE	REV BY INITIAL	DATE	TITLE	MODEL
CALC					FIBERGLASS BEAM SPAN = 20"	
CHECK						
APPD.						
APPD.						

U3 4013 8000 REV 1/66

REV LTR____

BOEING NO. FIGURE 12

SH.

1. REPRESENTS BEST OF 2240 CASES COMPUTED.
2. NUMBERS @ POINTS DENOTE BEAM DEPTH.
3. LATERALLY SUPPORTED @ 1/3 SPAN

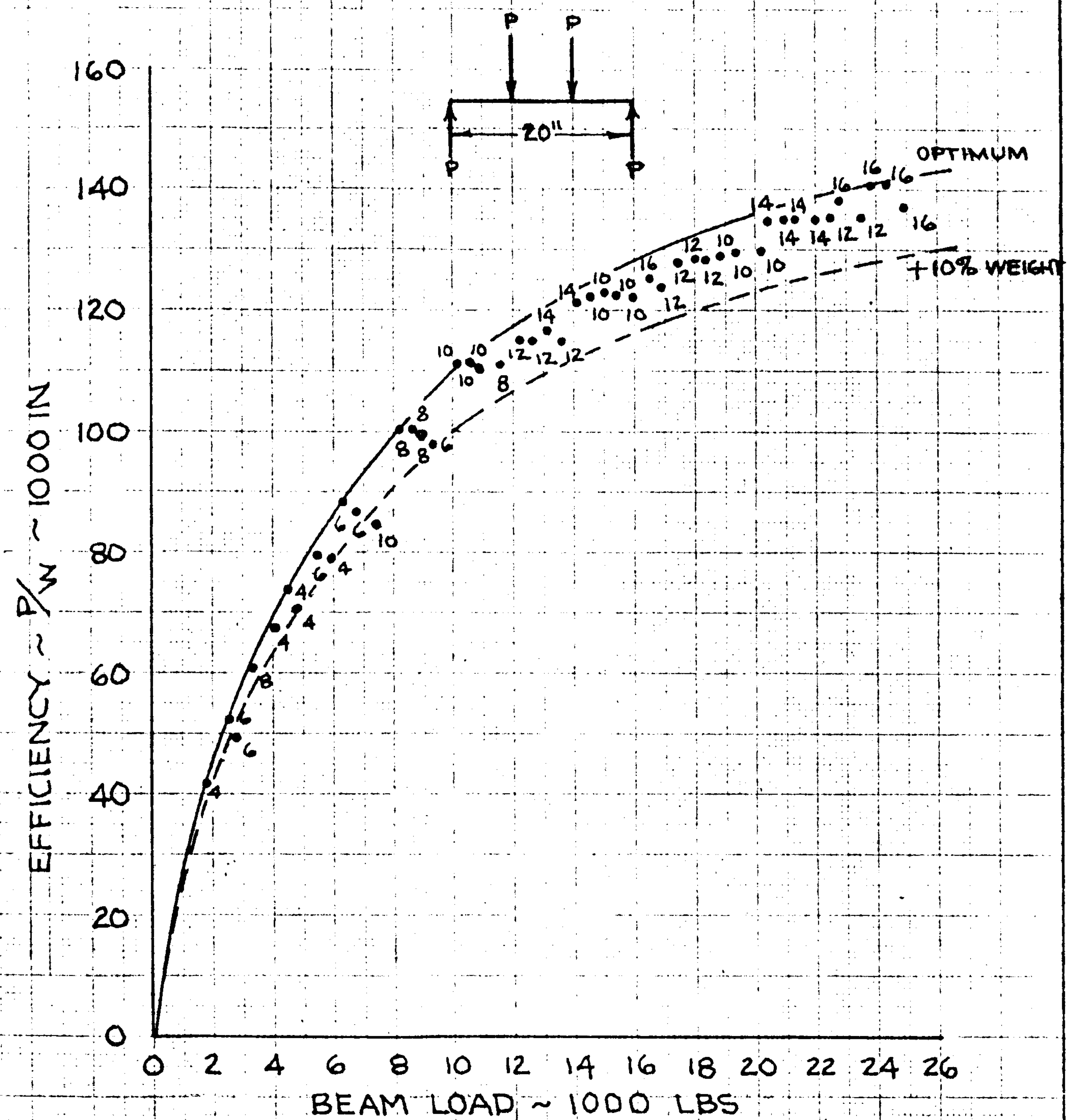

	INITIALS	DATE	REV BY INITIAL	DATE	TITLE	MODEL
CALC					7178-T6 ALUMINUM BEAM SPAN = 20"	
CHECK						
APPD.						
APPD.						

U3 4013 8000 REV 1/66

REV LTR____

BOEING NO. FIGURE 13

SH.

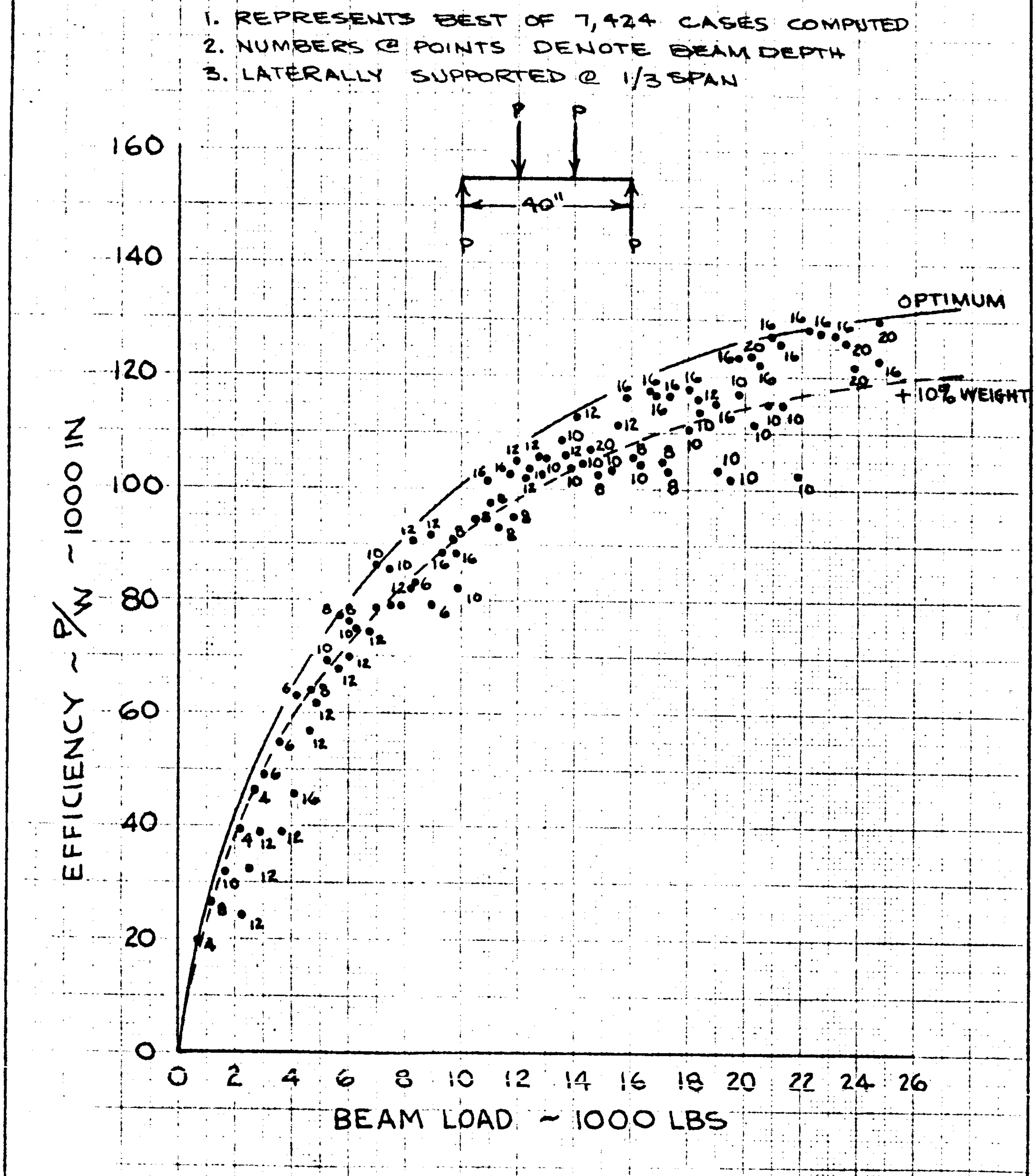

	INITIALS	DATE	REV BY INITIAL	DATE	TITLE	MODEL
CALC					FIBERGLASS BEAM SPAN= 40"	
CHECK						
APPD.						
APPD.						

U3 4013 8000 REV 1/66

REV LTR________

BOEING NO. FIGURE 14

SH.

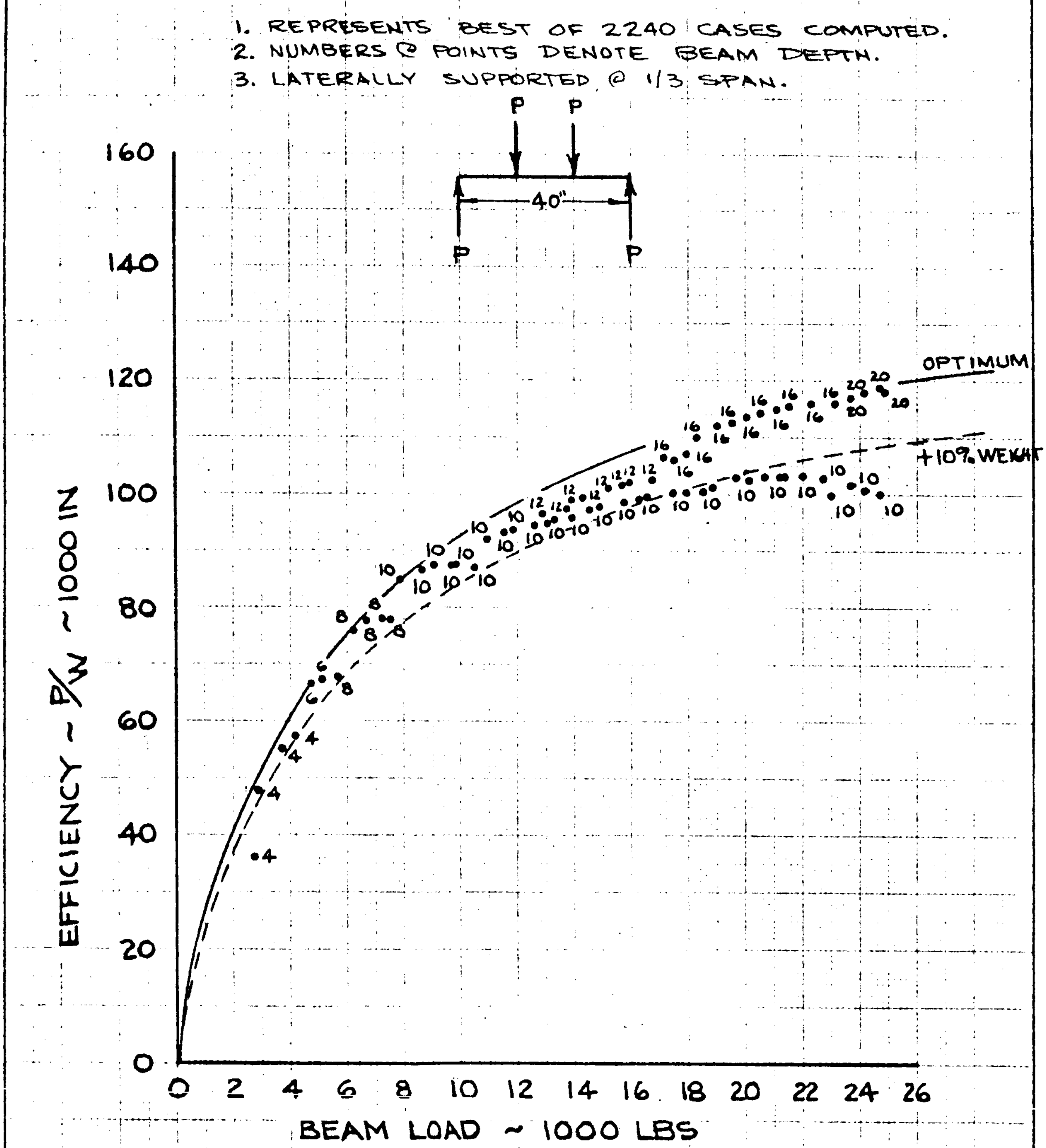

	INITIALS	DATE	REV BY INITIAL	DATE	TITLE	MODEL
CALC					7178-T6 ALUMINUM BEAM SPAN = 40"	
CHECK						
APPD.						
APPD.						

U3 4013 8000 REV 1/66

REV LTR

BOEING NO. FIGURE 15

SH.

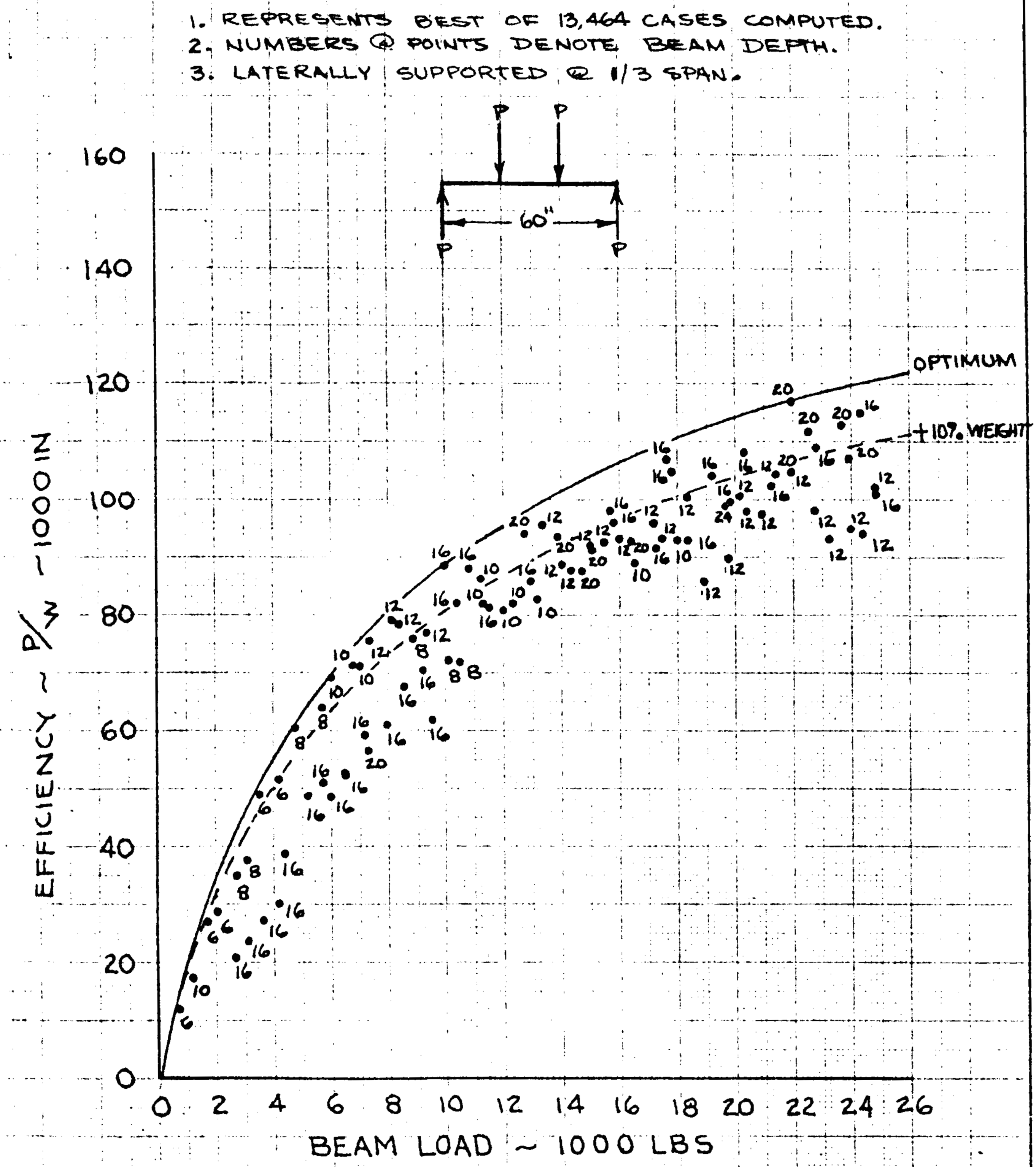

	INITIALS	DATE	REV BY INITIAL	DATE	TITLE	MODEL
CALC					FIBERGLASS BEAM	
CHECK					SPAN = 60"	
APPD.						
APPD.						

U3 4013 8000 REV 1/66

REV LTR

BOEING | NO FIGURE 16

SH.

1. REPRESENTS BEST OF 11,520 CASES COMPUTED.
2. NUMBERS @ POINTS DENOTE BEAM DEPTH.
3. LATERALLY SUPPORTED @ 1/3 SPAN

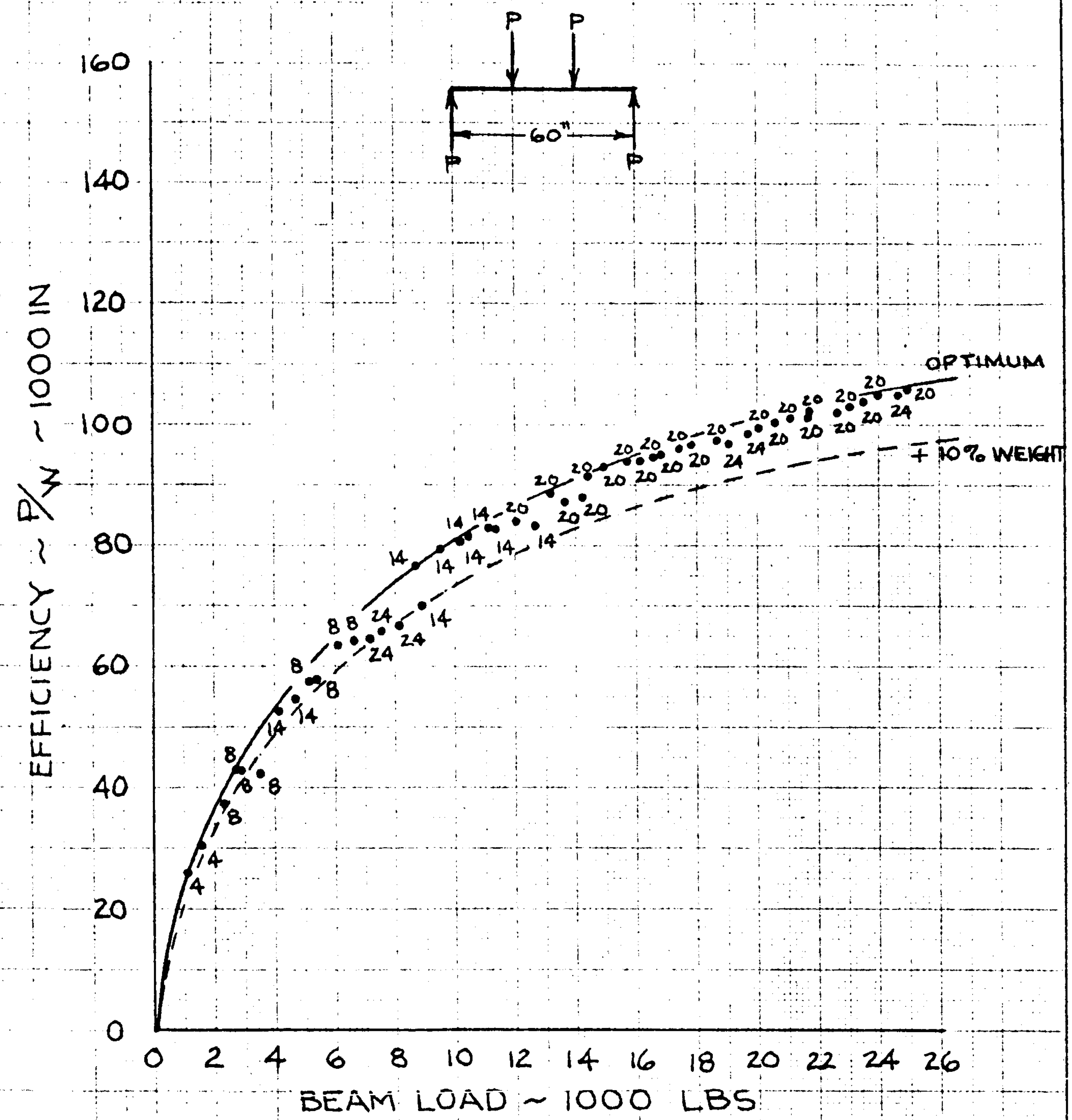

	INITIALS	DATE	REV BY INITIAL	DATE	TITLE	MODEL
CALC					7178-T6 ALUMINUM BEAM SPAN = 60"	
CHECK						
APPD.						
APPD.						

U3 4013 8000 REV 1/66

REV LTR________

BOEING | NO. FIGURE 17
SH.

1. REPRESENTS BEST OF 11,160 CASES COMPUTED.
2. NUMBERS @ POINTS DENOTE BEAM DEPTHS.
3. LATERALLY SUPPORTED @ 1/3 SPAN.

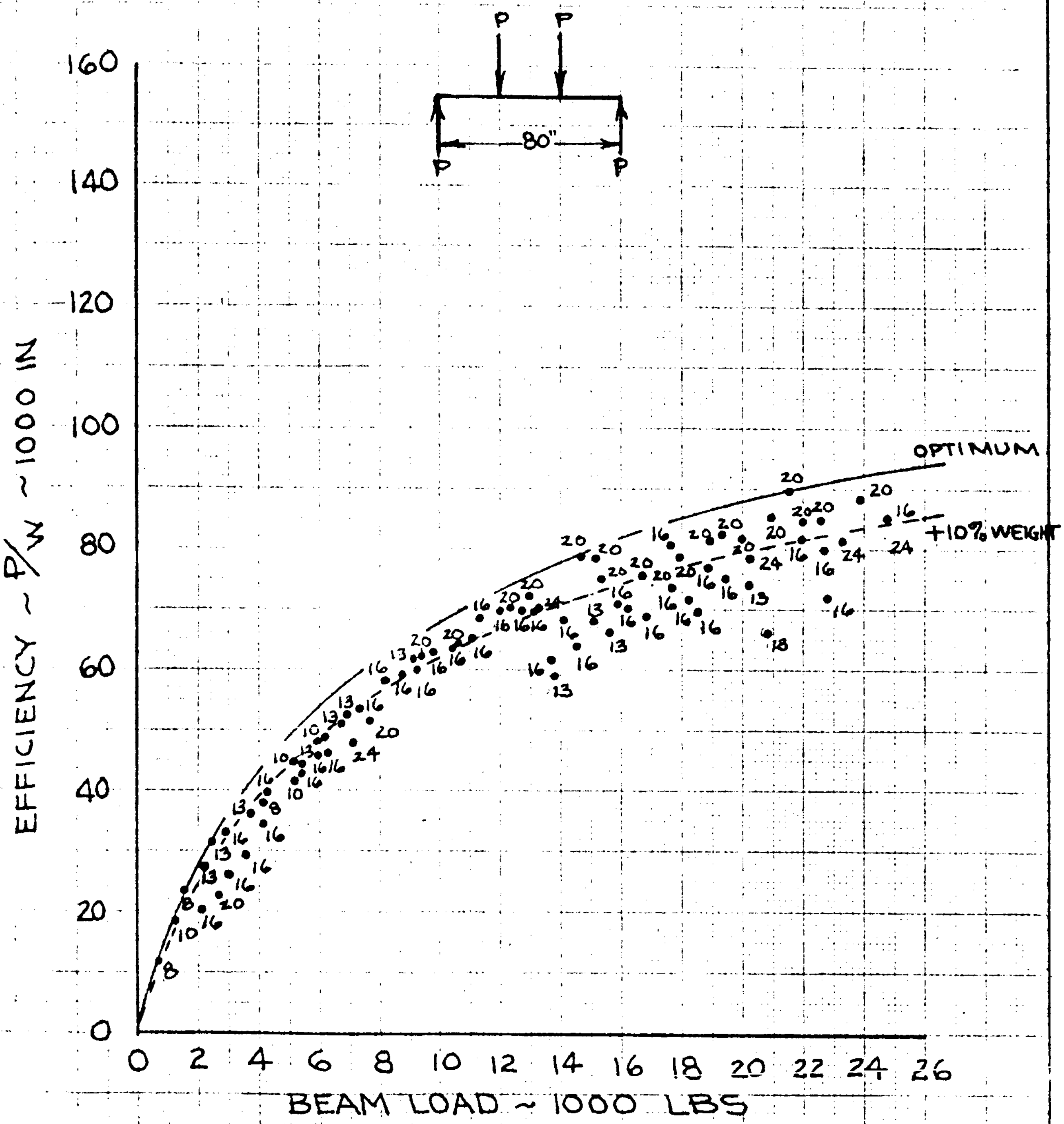

	INITIALS	DATE	REV BY INITIAL	DATE	TITLE	MODEL
CALC					FIBERGLASS BEAM SPAN = 80"	
CHECK						
APPD.						
APPD.						

U3 4013 8000 REV 1/66

REV LTR_______

BOEING NO. FIGURE 18
SH.

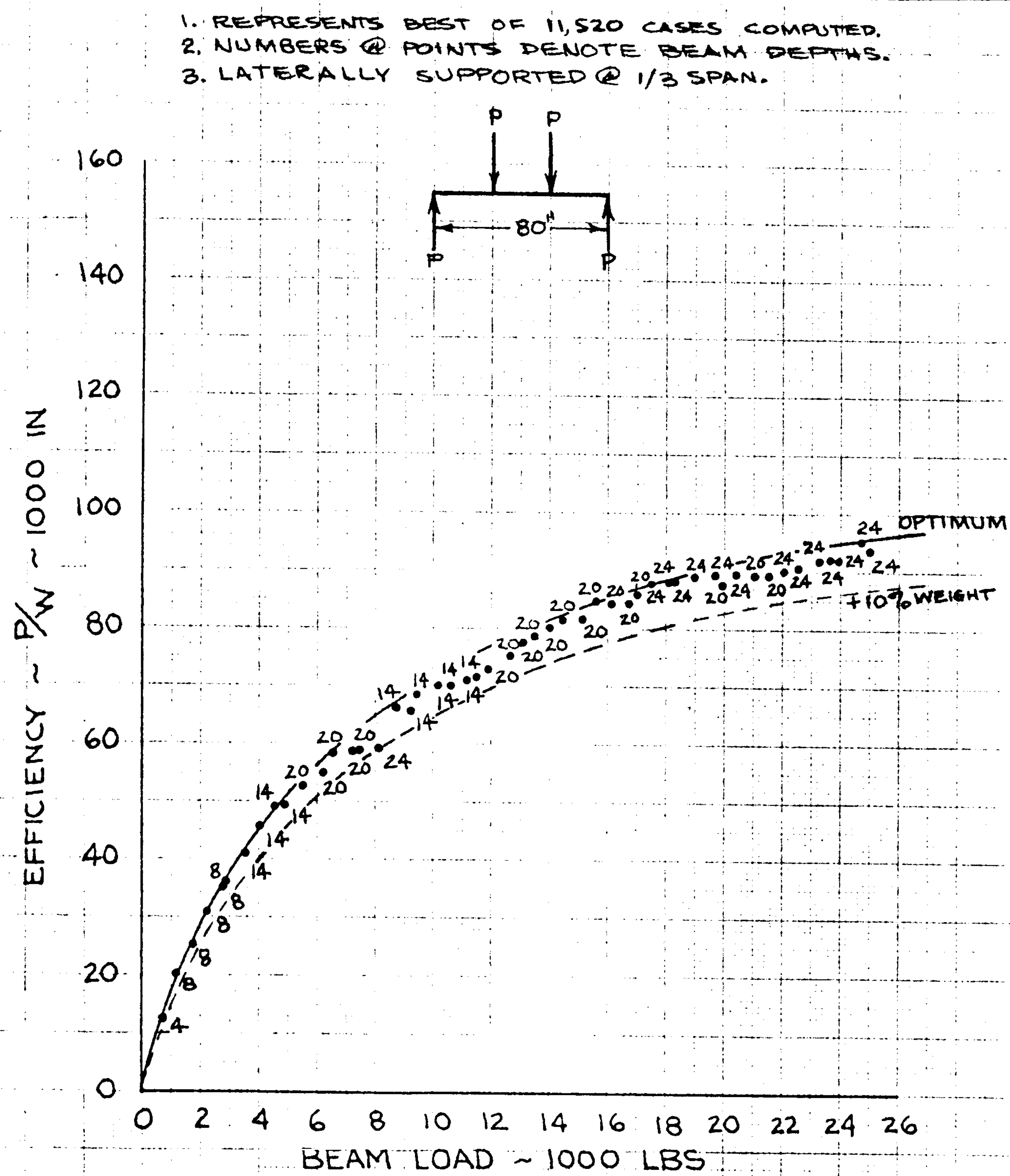

	INITIALS	DATE	REV BY INITIAL	DATE	TITLE	MODEL
CALC					7178-T6 ALUMINUM BEAM SPAN= 80"	
CHECK						
APPD.						
APPD.						

U3 4013 8000 REV 1/66

REV LTR

BOEING NO. FIGURE 19

SH.

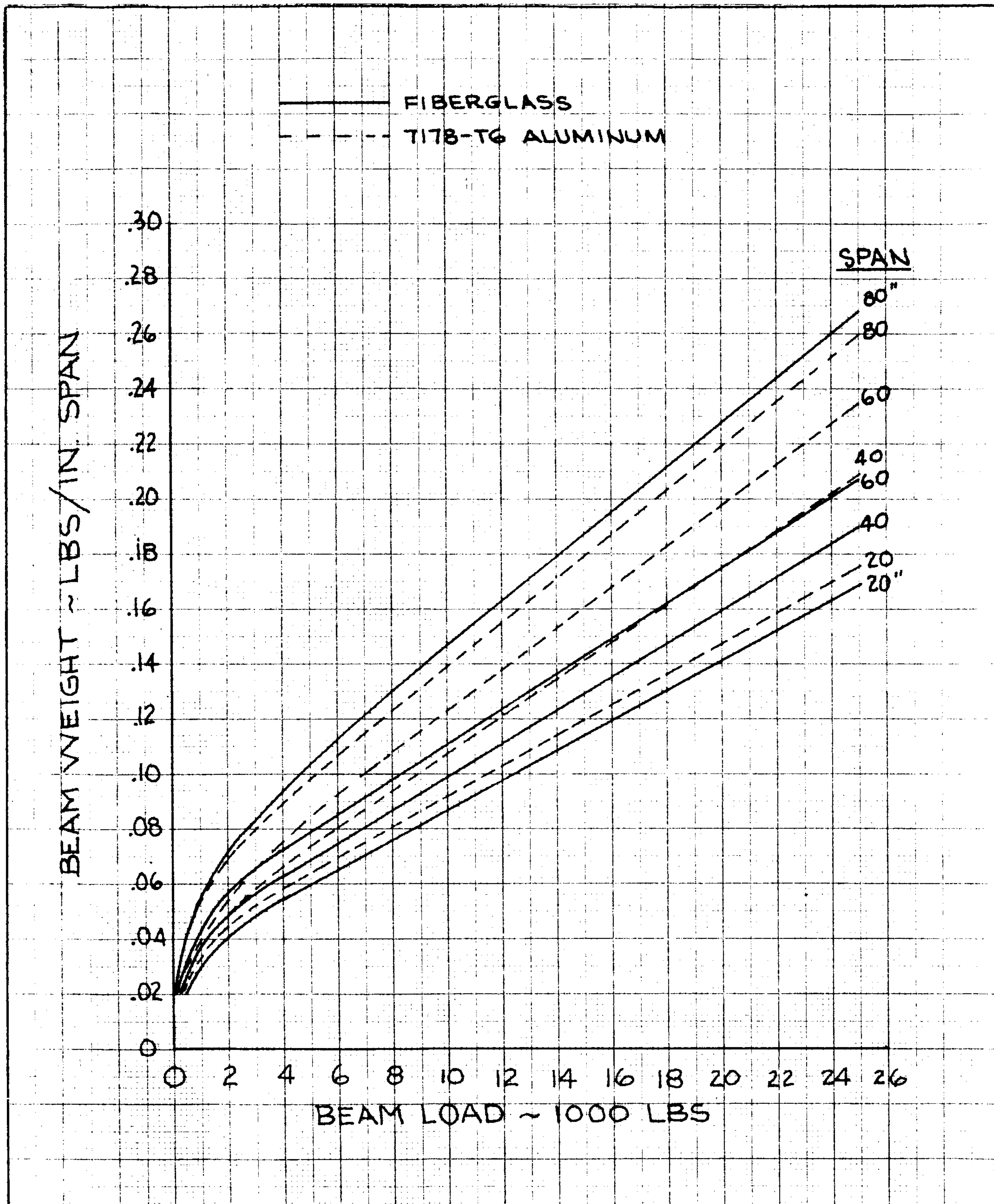

	INITIALS	DATE	REV BY INITIAL	DATE	TITLE	MODEL
CALC					BEAM WEIGHT COMPARISON FIBERGLASS & ALUMINUM	
CHECK						
APPD.						
APPD.						

U3 4013 8000 REV 1/66

REV LTR________

BOEING NO. FIGURE 20

SH.

advantage over the aluminum construction for spans of 20, 40, and 60". However, for the span of 80", the aluminum construction shows less weight than the fiberglass.

The weight differences are not appreciable. For instance, for a beam load of 10,000 lbs:

SPAN	WEIGHT DIFFERENCE
20	Alum. = 5.75% heavier
40	Alum. = 9.10% heavier
60	Alum. = 10.8% heavier
80	Fiberglass = 5.75% heavier

The inefficiency of the fiberglass in longer spans can be explained by the longer unsupported length of the compression flange and the low elastic modulus. Fiberglass flange lateral stability became critical in many of the cases as shown in Figure 10, whereas this mode of failure was not so predominant for the aluminum beams. It appears that use of high modulus filaments, such as graphite, would tend to make the nonmetallic beam more competitive with aluminum in the higher load ranges.

A comparison of beam weights derived by preliminary hand calculations (as shown in Figures 8 and 9 of the first quarterly report) and the rigorous computer analysis is shown in Figure 21.

The agreement is fair for the 20" span but is poor for the more highly loaded 60" span. The conclusions that were made from the preliminary design trade studies, however, are believed to be valid because (1) the same simplified analysis was used for all concepts investigated, and (2) the results from the computer analysis show the original evaluation of the honeycomb web construction to be conservative.

FIBERGLASS BEAM – HONEYCOMB WEB

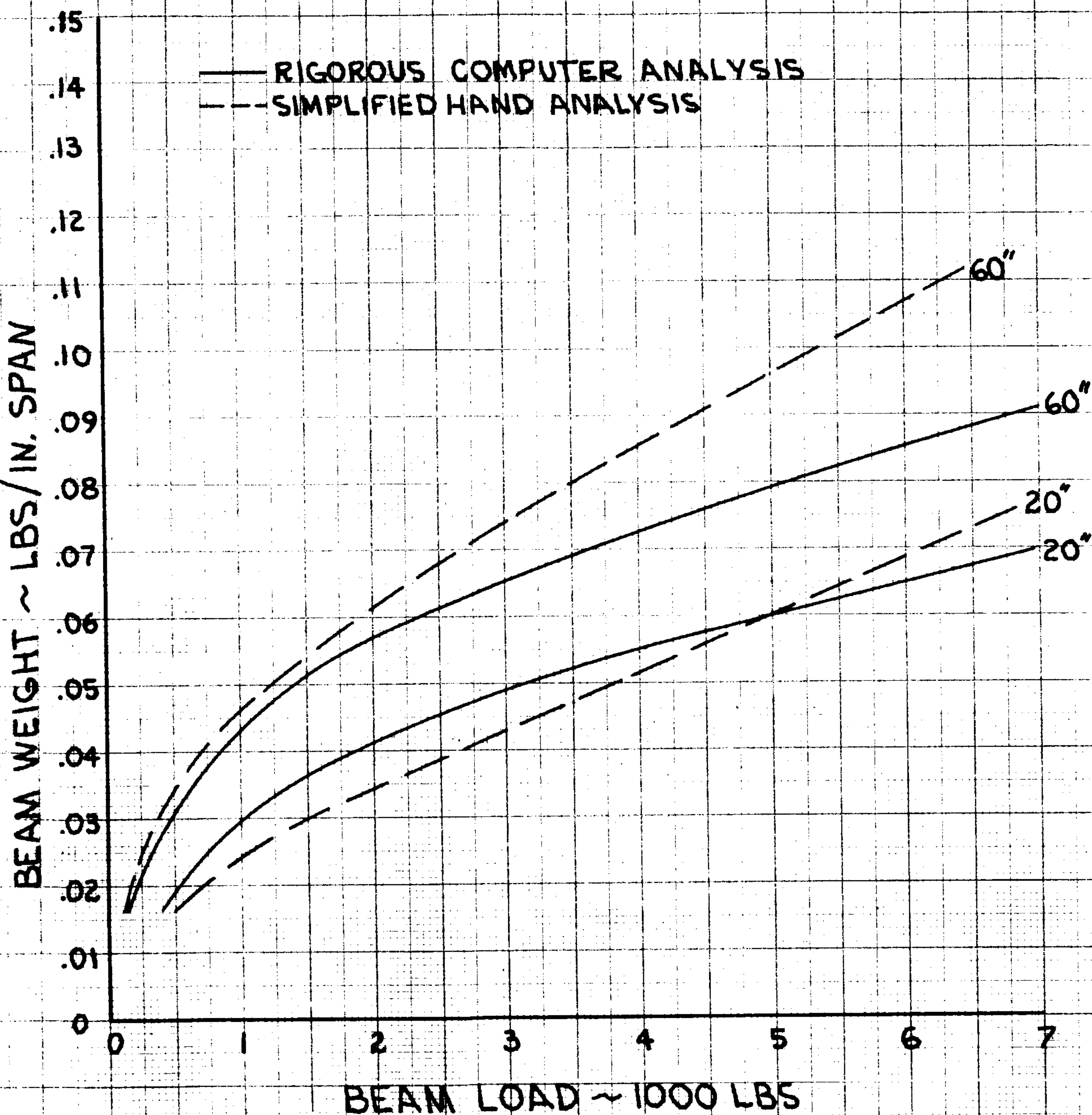

	INITIALS	DATE	REV BY INITIAL	DATE	TITLE	MODEL
CALC					BEAM WEIGHT COMPARISON – PRELIMINARY ANALYSIS VS. FINAL ANALYSIS	
CHECK						
APPD.						
APPD.						

U3 4013 8000 REV 1/66

REV LTR

BOEING NO. FIGURE 21
SH.

The results of the beam computer program are presently being studied to determine optimum geometries. A decision will then be made on the length of span to be fabricated and tested.

REFERENCES

1. Program for the Evaluation of Structural Reinforced Plastic Materials at Cryogenic Temperatures, L. W. Toth, et al., NASA/MSFC Contract NAS 8-11070, Goodyear Report GER 12792.